Supplementary Data

Supplementary Figure 1: MTM1 co-localizes with desmin in human muscle**.** Confocal analysis of transversal and longitudinal sections from two human control muscle biopsies (control 1 is 24 years-old and control 2 is 42 years-old) showing partial overlap between MTM1 and desmin at the sarcolemma and at the Z-disc. Scale bars = 50μm.

Supplementary Figure 2: (A) Desmin failed to immunoprecipitate MTM1 from cardiac muscle (right panel). Immunoblot of MTM1 in cardiac and skeletal muscle showed similar expression profile in both muscles (left panel). (**B**) Equivalent expression level of desmin and αB-crystallin in *Mtm1* vs. wild type cardiac muscle (upper panel). MTM1 knockout expression from heart did not affect desmin solubility. Sol indicates soluble fraction and Insol means insoluble material after final centrifugation (see methods) and solubilisation with 8M-urea extraction buffer (lower panel). GAPDH is a loading control. Data correlated from N=2 individual experiments and significance was set at *P< 0.05. (**C**) Transversal and longitudinal sections of wild type and *Mtm1* KO hearts stained with Haematoxylin and eosin (H&E) showed no myocardial fibrosis (myocyte injury and necrosis) in *Mtm1* KO muscle. All the analysed mice are 5 weeks old and *Mtm1* KO mice have the characterised severe muscle atrophy at that age. (**C**) LDH (lactate deshyndrogenase) and CK (creatine kinase) level in cardiac muscle from wild type and *Mtm1* KO mice. No variations were noted in these enzymes. Data correlated from two individual experiments (n=6 for wild type mice and n=7 for *Mtm1* KO mice) and significance was set at *P<0.05. Scale bars = 50μm.

Supplementary Figure 3: Mapping the interaction domains on MTM1 and desmin**.** (**A**) Diagrammatic representation of MTM1 deletion constructs employed in co-immunoprecipitation studies. (**B**) Co-immunoprecipitation using anti-MTM1 specific antibodies was performed from co-transfected cells with desmin and MTM1 full length or specified deletion constructs. Immune-bound complexes were analysed by immunoblot with anti-desmin antibody (top panel) and MTM1 antibody (bottom panel). MTM1D224-245 and MTM1D233-237 do not interact with desmin. (**C**) Co-immunoprecipitation studies employing anti-B10 antibodies from cells lysates co-transfected with desmin and B10 tagged wild type or mutated MTM1 constructs. Immune-bound complexes were revealed with anti-desmin antibody (top panel) and anti-MTM1 antibody (bottom panel). Levels of ectopically expressed desmin are shown

(middle panel). (**D**) Peptide mapping and competition to define the MTM1 binding domain. Top panel: Desmin overlay on MTM1 peptides encoding the 4 implicated loops (P1:MTM173-187, P2:MTM201-215, P3:MTM248-262, P4:MTM264-277), revealed with the desmin antibody. Bottom panel: MTM1-FL spotted on membrane was overlayed with desmin preincubated with excess of peptides (P1-P4). (**E**) Recombinant desmin alone or combined with specified mutated peptides was incubated with GST-MTM1 or GST. Coomassie blue stained gels showed GST and GST-MTM1 recombinant proteins (middle panel) and purified recombinant desmin (bottom panel) that were used for GST-pull down competition experiment. (**F**) Peptide mapping experiment using overlapping peptides of the 342-456 desmin sequence dotted on nitrocellulose membrane and overlayed by GST or GST-MTM1 recombinant proteins.

Supplementary Figure 4: Characterization of *Mtm1* knockdown C2C12 cell line and exploring desmin expression and localization in MTM1 deficient cells and muscle. (**A**) Expression of MTM1 and desmin during muscle cell differentiation employing MTM1 and desmin-specific antibodies (left panel). Quantification of mRNA levels of *desmin and Mtm1,* during myoblast differentiation was determined by quantitative RT-PCR compared to *Gapdh* or *Mhc* (right panel). (**B**) Characterization of *Mtm1* knockdown (KD) C2C12 cells. 3 clones were generated and 2 are presented here for protein and mRNA quantification comparatively to XLCNM myoblast carrying mutations leading to depletion (F238fs) or strong decrease (R241C) of MTM1 expression. Data correlated from N=3 individual experiments, n=3 separate cell culture extracts (middle and right panels) and significance was set at *$P < 0.05$. (**C**) Overexpression of desmin in *Mtm1* knockout (KO) muscle. Western blot analysis of muscle extracts from control and *Mtm1* KO muscles at 2 weeks and 5 weeks employing anti-desmin and anti-GAPDH specific antibodies. The 200-kDa bands detected by the desmin antibody in *Mtm1* KO muscle correspond potentially to a detergent-resistant desmin tetramer. Quantification of protein and mRNA levels of *Desmin* in control and *Mtm1* KO skeletal muscle (at 2 and 5 weeks). N= 4 individual experiments and n = 2 mice per experiment, significance was set at *$P < 0.05$. (**D**) Isolated fibres from *Mtm1* KO (2-weeks) muscle showed Desmin aggregates in the subsarcolemmal and intermyofibrillar compartments (arrowheads) compared to wild type muscle fibres. Scale bars represent 20μm.

Supplementary Figure 5: Specific accumulation of desmin in *Mtm1 KO* muscle. Immunolocalisation of syncolin, dystrophin, utrophin, α-actinin (Z-disc protein) and titin (M-line protein) in 2-week old control and *Mtm1* KO muscles. Accumulation of desmin was observed in *Mtm1* KO muscle fibers (arrowheads) but not the other tested protein. Scale bars represent 20μm.

Supplementary Figure 6: Impact of MTM1 on desmin filaments assembly**.** (**A**) MTM1 affects desmin filament structure. Recombinant desmin (10 μM) was mixed with increasing concentrations of recombinant MTM1 (cleaved from GST tag) and desmin filament assembly was monitored by electron microscopy after 60 min of assembly. Addition of MTM1 (4 μM) led to the formation of ribbon-like, bifurcating and branching filaments with more variable width and length. Excess of MTM1 (8-32 μM) inhibit completely filaments formation. (**B**) Desmin filament collapse/aggregation in *Mtm1* KO and knockdown myoblasts is not promoted by desmin phosphorylation. Immunoblot of desmin before (Total) and after elution from Ser/thr Phospho-enrichment column. ERK1/2 and GAPDH were analysed as positive and loading controls, respectively.

Supplementary Figure 7: Rescue of desmin filaments in *Mtm1* KO myoblasts. (**A**) Overexpression of wild type MTM1 but not mutated constructs (in the interaction sites with desmin) re-establishes normal desmin filament network in *Mtm1* KO myoblast (see also supplementary figure 7A). (**B**) XLCNM mutation R421Q and the artificial mutations S420D and C375S could re-establish normal desmin filament in *Mtm1* KO cells but not the XLCNM mutation R241C, suggesting that only MTM1 mutations situated in the interaction sites with desmin are not able to rescue desmin filaments network. (**C**) Quantification of the impact of all tested MTM1 mutations on filament network in *Mtm1* KO cells. Approximately 100 transfected cells were counted over 3 independent experiments. The significance was set at *P<0.05.

Supplementary Figure 8: Effects of MTM1 mutations on desmin filaments (**A**) Overexpression of wild type MTM1 but not mutated constructs (in the interaction sites with desmin) re-establishes normal desmin filament network in *Mtm1* Knockdown cells similarly to *Mtm1* KO cells (Supplementary Figure 7). (**B**) Overexpression of wild type MTM1 does not impact on desmin network in control C2C12 cells (Scramble) but overexpression of mutated MTM1 proteins carrying point mutations within the interaction sites with desmin (artificial or patient's mutations) lead to collapsed/aggregating desmin filaments. These mutated proteins may promote a dominant negative effect by binding the

endogenous MTM1 protein (**C**) and disrupting its interaction with desmin. Quantification of the impact of MTM1 mutations on filament network in C2C12 cells. Approximately 80 to 100 transfected cells per experiment were counted over 3 independent experiments. The significance was set at *P<0.05.

Supplementary Figure 9: Impact of MTM1 mutations in the desmin interaction sites on PIs phosphatase activity in vitro. (**A**) PtdIns(3,5)P_2 dephosphorylation to PtdIns5P by wild type or mutated MTM1 constructs (H181A, Y206A, S209A and K269A) alone or combined to desmin recombinant protein. (**B**) Coomassie blue stained gel of the MTM1 GST-fusion constructs employed for the enzymatic assay (right panel). (**C**) Quantification of the phosphatase activity: intensities of PtdIns5P and PtdIns(3,5)P_2 spots were measured at A(480/504) and expressed as a ratio on the recombinant protein quantity. Fluoremetric measurements were made twice and their averages were used. Data correlated from two individual experiments and significance was set at *P<0.05. (**D**) Desmin did not bind directly to lipids. A fat blot of specified lipids was overlayed with recombinant desmin (10 μg/ml), followed by probing with desmin specific antibodies.

Supplementary Figure 10: (**A**) MTM1 mutations fail to restore mitochondria network in *Mtm1* KO cells. Overexpression of wild type MTM1 but not mutated constructs (artificial and XLCNM mutations) did not rescue mitochondrial shape/network in *Mtm1* KO myoblast. (**B**) Quantification of the impact of MTM1 mutations on mitochondrial shape in *Mtm1* KO cells compared to MTM1 wild type (WT). Approximately 150 transfected cells were counted over 2 independent experiments. The significance was set at *P<0.05. (**C**). PtdIns(3,5)P_2 immunodetection in wild type and *Mtm1* KO/knockdown cells showed a similar profile as mitochondria. Perinuclear accumulation of PtdIns(3,5)P_2 and mitochondria in MTM1 deficient cells showed also partial overlapping between the PI and MitoTracker, suggesting a potential role of MTM1 substrate PtdIns(3,5)P_2 in mitochondrial homeostasis or a cytotoxic effect of PI accumulation on mitochondrial function.

Supplementary Figure 11. Disruption of MTM1-Desmin interaction does not impact on MTs and MFs networks. (**A**) Overexpression of wild type or mutated MTM1 constructs (that did not bind desmin) in C2C12 cells did not affect microtubules (MTs) and actin filaments (MFs) architecture. C2C12 cells tranfected with specified B10-tagged MTM1 constructs were processed with anti-B10 and anti-β tubulin or anti-actin antibodies. (**B**) The morphology of MTs and MFs of *Mtm1* KD C2C12 cells. Scale bar=50 μm.

Supplementary Figure 12: (**A**) Desmin and mitochondria collapse in XLCNM patient myoblasts, *Mtm1* knockdown cells and *Mtm1* KO muscle. Control vs. MTM1F238fs patient myoblasts and scramble vs. *Mtm1* KD cells were processed for imaging following incubation with MitoTracker red and anti-desmin specific antibodies. Desmin and mitochondria collapsed around nuclei in XLCNM and *Mtm1* KD C2C12 cells. (**B**) Desmin aggregates were present in *Mtm1* KD myotubes. Control or *Mtm1* KD C2C12 myotubes were processed for imaging with anti-desmin, anti-titin or anti-myotilin specific antibodies. Desmin formed aggregates in KD cells whereas, titin (A-I line) and myotilin (z-line) showed similar localisation between control and *Mtm1* KD myotubes. Scale bar=50 μm. (**C**) Mitochondria network is also altered in *Mtm1* KD myotubes with a specific accumulation between nuclei myotubes (arrowheads). Scale bar=50μm. (**D**) Subsarcolemmal and intermyofibrillar mitochondria are disorganised in *Mtm1* KO muscles. Longitudinal muscle sections from control and *Mtm1* KO mice were probed with anti-cytochrome *c* antibody. Mitochondria accumulation was detected in muscle transversal sections from *Mtm1* KO mice after injection with the RhodamineU6 probe. Scale bars=50 μm.

Supplementary Figure 13: Mitochondrial fission/fusion and susceptibility to apoptosis in *Mtm1* Knockdown cells are not affected. (**A**) Mitochondrial dynamics of control and *Mtm1* KD C2C12 cells were monitored over 300 sec by time-lapse microscopy (left panel). Quantification of mitochondrial fission and fusion events in control and *Mtm1* KD C2C12 cells (right panel). Mitochondria were counted individually in 3 distinct regions of the cell. Around 50 mitochondrial entities were scored as dividing (fission) or fusing (fusion) or neither (no event) per region from 9 control C2C12 cells (N=9) and from 11 *Mtm1* KD cells (N=11). Data correlated from 2 independent experiments and significance was set at $*P < 0.05$. (**B**) *Mtm1* KD did not impact on mitochondrial transmembrane potential. Control and *Mtm1* KD C2C12 cells were incubated with JC-1 and were analysed by FACS. Samples previously treated with 1μM staurosporine (STS) were also included in the assay. No significant shift in the profile of control versus *Mtm1* KD samples was observed. (**C**) Knockdown *Mtm1* in muscle cells did not increase susceptibility to apoptotic events. Control and *Mtm1* KD C2C12 cells were treated with (STS) and the morphology of their nuclei (stained with Höechst) was analysed by confocal microscopy (left panel). Cells with condensed or fragmented DNA (with or without STS treatment) were scored (right panel). Data correlated from 2 independent experiments using 4 different cell

batches. Approximately 120 cells were counted for each sample and significance was set at *P < 0.05.

Supplementary table 1: List of XLCNM patients carrying mutations compatible with prolonged life compared to the neonatal cases. Major part of these patients requires respiratory physiotherapy however no cardiac incidence or cardiac parameters defects were noted. (∗) A symptomatic female carrier (77-year-old) with restrictive respiratory dysfunction with a hemidiaphragmatic paresis, leading to death at 84 years of age. (#) Electrocardiogram showed repolarisation abnormalities. Echocardiogram disclosed pulmonary arterial hypertension (50 to 55 mm Hg), the right cavities were not dilated and there was no left dysfunction. Holter-ECG recorded bursts of supraventricular extra systoles.

Mutation (aa)	Recurrence	Phenotype, age	Respiratory support	Cardiomyopathy	Ref.
M1V	1	M, 5 yrs	Yes	NO	(1)
Y68D	1	M, 3 yrs	Yes	NO	(1)
L70F	2	M, 35 yrs	Yes	NO	(1)
N180K	1	M, 67 yrs	Yes at 55 yrs	NO	(1)
P226T	1	M, 12 yrs	Yes	NO	(1)
R241C	13	M, 11 yrs	Yes	NO	(1)
R241C	13	M, 7 yrs	Yes	NO	(1)
R241C	13	M, 10 yrs	Yes	NO	(1)
W346C	1	M, 3 yrs	Yes	NO	(1)
L498Stop (∗)	1	M, 84 yrs	Yes	(#)	(2)

Supplementary table 2. Primers used in this study for Q-PCR after reverse transcription. *Gapdh* and *Mhc* were used as standard controls.

GENE	Forward primers	Reverse primers	PCR (pb)
Mtm1	Catgcgtcacttggaactgtgg	Gcaattcctcgagcctcttt	235
Desmin	Gctctcaacttccgagaaacc	Tgtgtagcctcgctgacaac	121
Gapdh	Agctttccagaggggccatccaca	Ccagtatgactccactcacggcaa	444
Mhc	Gaacttgaaggagagaggtcga	Gatttaccaatgccttgtag	492

Supplementary movie 1. Time lapse (10 min) of mitochondrial motility in scramble C2C12 cells.

Supplementary movie 2. Time lapse (10 min) of mitochondrial motility in *Mtm1* KD C2C12 cells. Due to collapsed mitochondria in *Mtm1* KD cells, movies from both scramble and *Mtm1* KD cells were treated similarly with Imaris Imaging software (Bitplane Inc.) to track individual mitochondria.

SUPPLEMENTARY METHODS

Plasmid and constructs

Several constructs used in this study were subcloned into eukaryotic or prokaryotic vectors using the Gateway® recombination technology (Invitrogen, Carlebad CA, USA). The full-length open-reading frames for human *MTM1* (GenBank U46024), *MTM1*-GRAM (aa 1-162), *MTM1*-ΔGRAM (aa 146-603), *MTM1*-Cter (aa 545-603) were subcloned into the Gateway entry vector pENTR using BP recombination system as described by manufacture recommendation (Invitrogen). *MTM1* constructs were transferred to Gateway destination vectors for eukaryotic (pSG5 from Stratagene, with a tag corresponding to the B10 epitope of estrogen receptor) or prokaryotic expression (pGex4T3, Invitrogen). Human full-length desmin in pcDNA.3-*DESMIN* and pcDNA.3-*DESMIN*-myc vectors were kind gifts of Dr. P. Vicart and Dr. A. Lilienbaum (INSERM, Paris, France). For recombinant protein production, pDS5-*DESMIN* was kindly provided by Dr. H. Bar (Dep. of Molecular Genetics DKFZ, Heidelberg, Germany). Human Neurofilament Light-chain vector pcDNA 3.1/myc-His vectors (Invitrogen) was a gift from Dr. A. Bolino (Milano, Italy) and Sumo cDNA was a gift from Dr. F. Klein (IGBMC, Illkirch, France). The panel of deletions and amino acid changes was engineered by PCR-based mutagenesis from the cDNA encoding the wild-type protein (MTM1 or Desmin) using Deep vent DNA polymerase (Ozyme) or PFU DNA polymerase (Agilent technologies). All constructs were verified by sequencing.

Antibodies

Monoclonal anti-MTM1 antibody 1G1 and polyclonal antibodies 2347 and 2827 were generated and characterized previously (3-5). A new polyclonal antibody (2868) was produced and directed against the mouse MTM1 C-ter end (cys-TSSSSQMVPHVQTHF). Anti-B10 and anti-Myc monoclonal antibodies were home engineered (IGBMC, Illkirch-France). Monoclonal anti-titin, monoclonal anti-myotilin and anti-pan plectin antibodies were kindly provided by Dr. D. Mornet (ERI25, INSERM, Montpellier, France). Anti-frataxin antibodies were provided by Dr. H. Puccio (IGBMC, Illkirch, France). The following commercial antibodies were used in this study: Mouse monoclonal anti-desmin antibody (clone D33) (DAKO, Germany), mouse monoclonal anti-αB-crystallin (clone 1B6.1-3G4, Stressgen, assay designs), mouse monoclonal anti-α-actinin, mouse monoclonal anti-actin, mouse anti-GAPDH

(clone 6C5) (Euromedex, France), mouse anti- PtdIns(3,5)P_2 (Echelon Biosciences Inc.) and mouse anti-Phospho ERK1/2 (Cell signalling Inc.), polyclonal antibodies anti-desmin (Y20), rabbit polyclonal antibody anti-Myc, rabbit anti-prohibitin (Abcam, Cambridge), rabbit anti-cytochrome C (Santa Cruz Biotechnology, Inc.). For peroxidase coupled secondary antibodies goat anti-mouse, goat anti-rabbit and donkey anti-goat antibodies were from Jackson ImmunoResearch Inc (England).

Yeast Two-hybrid

Yeast two-hybrid screening was performed by Hybrigenics, S.A., (Paris, France) (http://www.hybrigenics-services.com). The coding sequence for amino acids 150-603 of human *MTM1* (GenBank accession number gi: 4557896) was PCR-amplified and cloned into pB27 as a C-terminal fusion to LexA (N-LexA-MTM1-C) and into pB66 as a C-terminal fusion to Gal4 DNA-binding domain (N-Gal4-MTM1-C). The constructs were checked by sequencing the entire insert and used as a bait to screen a random-primed human adult/fetal skeletal muscle cDNA library constructed into, pB27, pB66 and pP6 vector derived from the original pBTM116 (6), pAS2ΔΔ (7) and pGADGH (8) plasmids, respectively. For the LexA bait construct, 89 million clones (9-fold the complexity of the library) were screened using a mating approach with Y187 (matα) and L40ΔGal4 (mata) yeast strains as previously described (7). For the Gal4 construct, 99.6 million clones (10-fold the complexity of the library) were screened using the same mating approach with Y187 (matα) and CG1945 (mata) yeast strains. A total of 49 His+ colonies were selected on a medium lacking tryptophan, leucine and histidine, and supplemented with 0.5 mM 3-aminotriazole (only for the Gal4 screen) to handle bait autoactivation. The prey fragments of the positive clones were amplified by PCR and sequenced at their 5' and 3' junctions. The resulting sequences were used to identify the corresponding interacting proteins in the GenBank database (NCBI) using a fully automated procedure. Four clones encoding the Human class III intermediate filament desmin were identified in the initial screen.

GST-fusion proteins production and pull down

MTM1 constructs (full-length, ΔGRAM, GRAM, C-ter) were transferred by recombination into the Gateway pGex4T3 vector and transformed into BL21-Rosetta 2 strain (Novagen). For negative control the empty pGex4T3 vector (GST alone) was used. Bacteria were grown in 2X-YT (1% Yeast extract, 1% bactotryptone, 2,5mM NaOH and 0,5% NaCl) enriched medium until mid-log phase (OD reaches

0.5). Induction was performed with 1mM IPTG at 16°C during 12 hr. Recombinant proteins were extracted from cell pellets with lysis buffer (50mM Tris-Cl pH 8.0, 100mM NaCl, 1mM EDTA). Fresh DTT (1mM), PMSF (1mM) and complete protease inhibitor tablet (Roche) supplemented with 1mM Leupeptin and 1mM pepstatin A (SIGMA). Lysozyme (SIGMA) was added to 1mg/ml and bacteria were incubated on ice and mixed occasionally by inversion. To increase solubility of recombinant proteins we added 0,1% Sarcosyl and 0,5% of Triton X-100 and mixed in rotamixer at 4°C overnight. Bacterial lysates were spun down at 20,000 rpm and supernatants containing soluble proteins were loaded onto a Gultathione Sepharose resin (GE-Healthcare) overnight at 4°C. Bound GST-fusion proteins were washed with lysis buffer 4 times and ones with lysis buffer adjusted to 500 mM NaCl. Purified GST-fusion protein-beads were submitted to final washes in lysis buffer without NaCl. Non-transfected and transfected COS-1 cells with pcDNA3.1-desmin (see cell culture and tranfection) were homogenized with ice-cold low-salt Tris buffer (10mM Tris-Cl pH 7.6, 140 mM NaCl, 5mM EDTA, 5mM EGTA, 0,5% Triton X-100, 2mM PMSF). After centrifugation the insoluble material was resuspended in ice-cold high-salt buffer (10mM Tris-Cl pH 7.6, 1,5 M KCl, 140 mM NaCl, 5mM EDTA, 5mM EGTA, 0,5% Triton X-100, 2mM PMSF), homogenised and pelleted by centrifugation. The resulting pellet was washed with the same buffer without KCl and NaCl to remove excess of salt and solubilised again in ice-cold low salt Tris buffer to get high amount of soluble desmin. The same procedure was applied to C2C12 myotube homogenates and also to muscle homogenate using a Dounce homogenizer. The resulting homogenates were mixed with GST-fusion MTM1-beads and incubated at 4°C for 4 to 12 hr. After several washes with the low-salt Tris buffer, beads were resuspended in Laemmli buffer, heated for 3 min at 95°C, and proteins were separated by SDS-PAGE. Desmin was revealed with corresponding specific antibodies described above.

Co-immunoprecipitation

The entire procedure was carried out at 4°C. Whole cell extracts from COS-1 (co-transfected with specified constructs) and C2C12 myotubes were obtained by homogenization in Co-IP buffer (50 mM Tris-Cl pH 7.5, 100 mM NaCl, 5mM EDTA, 5mM EGTA, 1mM DTT, 0,5% Triton X-100, 2mM PMSF) supplemented with complete protease inhibitor tablet (Roche) and 1mM Leupeptin and 1mM pepstatin A (Sigma). Cells were homogenized in a Dounce homogenizer and passed five times through 25G needle to disperse aggregates. After centrifugation (7000 g, 10 min) the insoluble material was frozen

in liquid nitrogen and submitted twice to the same extraction procedure with Co-IP buffer. All soluble fractions were pooled to have optimal levels of proteins of interest. For whole muscle lysate preparation, fresh *tibialis anterior* muscles were dissected from adult mice and homogenized with a Dounce homogenizer in ice-cold Co-IP buffer supplemented with 0.05% (w/v) SDS. Cycles of 10 min homogenization spaced by 10 min incubation on ice were repeated 3 times. After 30 min centrifugation at 30,000 rpm, pellets were treated by 2 cycles of freeze-thaw in ice and homogenized as described above in small volumes. Finally the supernatants were pooled for the pull-down experiment. Soluble homogenates (from cells or muscle) were pre-cleared with 50 ml of G-sepharose beads (GE-Healthcare) for 1 hr and supernatants were incubated with the specific antibodies directed against the protein of interest or against the fusion tag (B10 and Myc) at 4°C for 12 to 24 hr. Protein G-sepharose beads were then added for 4 hr to capture the immune complex. Beads were washed 4 times with Co-IP buffer and 2 times with high stringency co-IP buffer (with 500 mM NaCl). For all experiments, two negative controls consisted of a sample lacking the primary antibody and a sample incubated with another primary antibody from the same serotype as the antibody of interest. Resulting beads were eluted with Laemmli buffer and submitted to SDS-PAGE followed by western blot.

Desmin purification

For the expression and purification of desmin, BL21-Rosetta-2 bacteria were transformed with pDS5-*DESMIN* and the isolation of inclusion bodies were performed according to the initial protocol of Nagi and Thogerson with the modification provided by Herrmann et al. (9). After resuspension of bacterial pellets with the Dounce homogenizer, we added 0.2% Triton X-100 followed by 10 mM MgCl2, 50 mg/ml DNAase I (Roche) and 2 mM PMSF. The permeabilized bacteria were gently agitated with tight-fitting pistil until the viscosity of the solution was low and the inclusion bodies were harvested by centrifugation, resuspended in the corresponding washing buffer, and successively transferred back to the Dounce homogenizer pre-cooled on ice. Inclusion bodies were homogenized with KCl-Tris buffer (10 mM Tris-Cl pH 7.5, 1 mM EDTA, 1 mM DTT, 2 mM PMSF and 1.5 M KCl). After centrifugation this procedure was repeated with the same buffer without KCl (Tris buffer). Finally the pellet was homogenized in 10 mM Tris pH 7.5 and 0.1 mM EDTA to remove salt. The pellet from the last centrifugation was dissolved in 10 mM Tris-Cl, pH 7.5 with 9.5 M Urea. Solubilised desmin was collected by centrifugation at 100,000 g for 1 hr at 20°C and the resulting supernatant was submitted

to column purification. Desmin was passed through Fast-flow DEAE-Sepharose (SIGMA) equilibrated with column buffer (10 mM Tris-Cl pH 7.5, 1 mM DTT and 8 M urea). Econo-columns (Bio-Rad) were used. Bound proteins were eluted by a salt gradient (0-300 mM Nacl) in column buffer and fractions were analysed by SDS-PAGE. Peak fractions were pooled, diluted to decrease salts and directly applied to a CM-Sepharose (SIGMA) equilibrated with column buffer. Purified desmin was eluted by gradient salt as described above and analysed by SDS-PAGE. To avoid protein carbamoylation, all urea buffers were stirred in the presence of a mixed-bed ion exchanger resin (TMD-8, M8157, SIGMA). To obtain soluble complexes, desmin filaments were dialyzed in steps of decreasing urea concentration (6M, 4M, 2M) for 1 hr dialysis period at RT (weight cut off of 10,000 Dalton). The solubilisation-dialysis buffer (5 mM Tris-HCl pH 8.4, 1 mM EDTA, 0.1 mM EGTA, and 1 mM DTT) was used as buffer for all steps and for the final dialysis to remove traces of urea. Finally, desmin filaments were dialyzed overnight at 4 °C.

Electron microscopy and negative staining

To visualize desmin filaments, desmin was solubilised at 0.4 mg in solubilisation buffer and assembly was started by the addition of an equal volume of filament buffer (45 mM Tris-Cl pH 7.0 and 100 mM NaCl). Filament assembly was performed at RT and samples were taken at 10 seconds, 5 min, 10 min, and 60 min). Assembly was stopped by the addition of the same volume of assembly buffer (25 mM Tris-Cl pH 7.5, 50 mM NaCl) containing 0.2 % glutaraldehyde (SIGMA). 5-8 µl of protein suspension was then delivered to a glow-discharged, carbon coated copper electron microscopy grid (10, 11). Filaments bound to the support were washed with distilled water and stained by incubation with 2% uranyl acetate for 15 seconds. The staining solution was removed and the grid was air dried and observed under a Philips CM120 transmission electron microscope operating at 100 kV with a LaB6 filament. Areas covered with molecules were recorded under low dose condition, at a magnification of 100 nm on a Pelletier cooled CCD camera (Model 794, Gatan, Pleasanton, CA). Measurement of filaments length and diameter was performed on images enlarged five times from the original images (from at least 2 independent experiments) using Image J software (National Institute of Health, USA). To assess the impact of MTM1 on desmin filament, GST-MTM1, GST-MTM1S209A and GST-Sumo (control) were purified as described before and GST was cleaved by thrombin (SIGMA).

Recombinant proteins were dialysed against desmin solubilisation buffer (see above) and mixed with desmin at equimolar ratio (or using increasing amount of MTM1) before starting filament assembly.

Co-sedimentation assays

Effect of MTM1 on desmin assembly was also investigated by a sedimentation assay (10) with the following modifications. Briefly, desmin (10 μM) was incubated at 37°C in assembly buffer for 1 hr with GST-MTM1 (GST-MTM1S209A and GST alone were used as controls) at the same concentration (10 μM each). The mixtures were centrifuged at 100,000 g for 10 min and identical volumes of supernatant and pellet were subjected to SDS-PAGE followed by Coomassie blue staining. The second experiment consisted to increase the amount of GST-MTM1 (4, 8 and 16 μM) mixed with desmin to test the impact on polymerisation. Samples were centrifuged and analysed as described above. Gels were scanned to quantify the fraction of GST-MTM1 and desmin in pellet and supernatant fractions.

Western and far western blots

Protein samples were homogenized in Laemmli buffer, boiled 5 min at 95°C, separated on 10% SDS-polyacrylamide gels and transferred onto nitrocellulose membranes (Schleicher and Schuell). After blocking the membranes overnight at 4 °C in 5% milk in TBST, primary antibodies were applied at the specific dilution in 5% milk in TBST buffer and incubated for 1 hr at RT or overnight at 4°C depending on the specificity of the antibodies and manufacturer's instructions. The membranes were washed 5 times with TBST, and horseradish peroxidase-conjugated secondary antibodies (Jackson Immuno Research Laboratories) were applied for 1 hr. After 5 times washing with TBST, membranes were developed using superSignal west Pico kit (Thermo scientific, PEIRCE) following the manufacturer's instructions. For far western experiments, nitrocellulose membranes were preincubated 15 min with fresh 1X probe dilution buffer from (PBS, 0.3% BSA, 0.1% goat serum) as described (12). Protein probes were diluted in the appropriate concentration in the 1X probe dilution buffer and incubated on the nitrocellulose for 2 hr at RT. After four washes with PBS, the membrane was blocked with 5% milk in TBST for 1 hr at RT and incubated with the primary antibody followed by the horseradish peroxidase-conjugated secondary antibody, and finally revealed as described above.

Peptides and dot blot

All peptides were 9-Fluorenylmethyloxycarbonyl (Fmoc) coupled (Peptide synthesis platform, IGBMC, Illkirch, France) and synthesized using solid phase 431A or 433A automatic synthesisers (Applied Biosystem). Peptides were purified by HPLC and verified by mass spectrometry. For dot blot, diluted peptides at the indicated concentration were spotted on a 0.2 μM nitrocellulose membrane using Bio-Dot SF microfiltration apparatus (Bio-Rad, France) following the manufacturer's instructions. Purified recombinant proteins were applied at the described dilutions and spotted membranes were incubated with the primary antibody followed by the horseradish peroxidase-conjugated secondary antibody and finally revealed using superSignal west Pico kit (Thermo scientific, PIERCE). For competition experiments, recombinant proteins were pre-incubated with competitor peptides for 1-12 hr at 4°C before the incubation step with spotted nitrocellulose membrane.

Stable *Mtm1* knockdown cell generation

Knockdown (KD) *Mtm1* and control C2C12 cells were generated in triplicates following the protocol used by Dalkilic et al. (13). Potential sites for siRNA sequences were identified using the BD Biosciences Clontech RNAi Designer (http://bioinfo.clontech.com/rnaidesigner/) and Invitrogen's BLOCK-iT RNAi Designer (https://rnaidesigner.invitrogen.com/rnaiexpress/). The targeted sequence sites were used to design the hairpin sequences for insertion into the pSirenRetroQ vector (BD Biosciences). The following sequence was used: ACGGATTCTGCTCTAATAC for mouse *Mtm1*. Forward (GAT CCA CGG ATT CTG CTC TAA TAC TTC AAG AGA GTA TTA GAG CAG AAT CCG TTT TTT TGC TAG CG) and reverse (AAT TCG CTA GCA AAA AAA CGG ATT CTG CTC TAA TAC TCT CTT GAA GTA TTA GAG CAG AAT CCG TG) primers were synthesized, annealed, and ligated to the pSirenRetroQ vector using the EcoRI and BamHI restriction sites according to the manufacturer's protocol. Plasmids were then transfected into the 293E (ecotropic) packaging cell line using Lipofectamine 2000 reagent (Invitrogen). The resulting viruses were harvested after 2 days, passed through a 0.45-*μ*m-pore-size filter to remove any detached cells. C2C12 cells were plated on six-well plates (50,000/well), and a day later, the viruses were mixed with Polybrene and incubated with the cells for 15 min. The plates were centrifuged for 30 min at 37°C, at 2500 rpm, and the viral supernatant was then removed. The next day, infected cells were plated in selection medium containing puromycin (2.5 μg/ml).

Generation of adeno-associated virus (AAV)-*Mtm1* and intramuscular delivery

Mouse *Mtm1* cDNA (AF073996 [GenBank], NCBI) was cloned into a pENTR1A Gateway entry vector (Invitrogen), and then recombined into the pAAV destination vector. Viral particles were produced and purified as previously described (3) with the following modification. Production and purification of AAV constructs for transduction was performed by the Genetic Engineering platform of the IGBMC (Strasbourg, France). Adenovirus-free pseudotyped AAV2/1 preparations were generated by tri-transfection of AAV-293 cells with the plasmids pAAV2-insert, pAAV-RC (plasmid which contains the AAV2 rep and AAV1 or 2 cap genes), and pHelper (encoding adenovirus helper functions). Recombinant vectors were purified by double cesium chloride ultracentrifugation gradients from cell lysates or by affinity onto Heparin column, followed by dialysis against sterile PBS and concentration. Physical particles were quantified by real time PCR and vector titers are expressed as viral genomes per ml (vg/ml). rAAV titres used in these experiments were $5\text{-}7\times10^{11}$ viral genomes per ml (vg/ml). 5 to 6 week-old *Mtm1* KO mice were anesthetized by intraperitoneal injection of 5 µl/body gram of ketamine (20 mg/ml, Virbac) and xylazine (0.4%, Rompun, Bayer). Tibialis anterior (TA) muscles were injected with 25 µl of AAV-*Mtm1* or AAV preparations or with sterile PBS solution. Animals were housed in a temperature-controlled room (19–22°C) with a 12:12-h light/dark cycle. Mice were humanely killed by CO_2 inhalation followed by cervical dislocation. TA muscles were dissected 2-4 weeks after injection and frozen in nitrogen-cooled isopentane and liquid nitrogen for histological and immunoblot assays, respectively. Care and manipulation of mice were performed in accordance with national and European legislations on animal experimentation, and approved by the institutional ethical committee.

Cell culture, transfection and immunofluorescence

COS-1 cells were grown in Dulbecco medium supplemented with 5% FCS. C2C12 mouse myoblast cells (control and *Mtm1* KD) were maintained in Dulbecco medium supplemented with 20% FCS for proliferation and differentiated by adding the differentiation medium (Dulbecco medium + 5% HS). Cells were then left from 2 to 9 days to differentiate into myotubes. Human and mice primary myoblast cultures were generated from human biopsy explants and 2 weeks-old mice. Briefly, after a cell proliferation phase from muscle explants, harvested cells were then sorted by FACS using an anti-CD56/NCAM antibody (for Human cells) and anti-CD34+ (for mice cells) the selected cells were left for

proliferation in Dulbecco medium supplemented with 20% FCS and 2% Ultroser G (Biosepra). Characterization of the XLCNM patients cells used in this study was previously reported (14). Cells were differentiated into myotubes by decreasing FCS in the medium to 2%. All cell culture media were supplemented with gentamyncin (400 U/ml). In the case of C2C12 control and *Mtm1* KD cells, 2 μg/ml puromycin were added to the medium for selection as mentioned above. COS-1 cells were transfected with Fugene 6 (Roche, France) and C2C12 cells with Lipofectamine 2000 (Invitrogen) according to the manufacturer's instructions. For immunofluorescence, cells were grown on glass coverslips (Nalge Nunc Inc.) and transfected with the appropriate DNA. To observe mitochondria, cells were incubated for 10 min with Mitotraker Red (Molecular probes, Invitrogen) diluted in culture medium. After fixation with 4% paraformaldehyde or cold methanol and saturation with fetal calf serum, cells were permeabilized and incubated with the appropriate primary antibodies. Samples were washed and incubated with goat anti-mouse or goat anti-rabbit or donkey anti-mouse or donkey anti-rabbit secondary antibodies coupled to Alexa fluor488 or Alexa fluor595 (Invitrogen) and observed with a Leica DM microscope for epifluoresence or with a Leica SP2 MP confocal microscope.

Time-lapse microscopy

Cells incubated with MitoTraker were washed with culture medium twice prior to analysis. Cells were observed during 10 min using the Leica DM IRE2 videomicroscope and Leica SP5 confocal video-microscope. Cells were maintained at 37 °C in a sealed observation chamber during image acquisition. Short exposure time and a neutral density filter were used to minimize photobleaching and phototoxicity. Collection of image stacks was produced using the Metamorph Imaging System (Universal Imaging Corp, Downingtown, PA, USA) or Imaris Imaging software (Bitplane Inc.). To avoid measuring movement due to cell retraction, only cells that did not move during the observation were analysed. Individual mitochondria spots were tracked using Image J software (National Institute of Health, USA) and vector lengths (movement of particles between two consecutive frames) were exported to Microsoft Excel and the velocities of the particles were calculated in μM/second.

Electron microscopy

C2C12 cells (*Mtm1* KD and control) were fixed in 2.5% gluteraldehyde with 0.1M sodium cacodylate buffer (PH 7.2) for 24 hr at 4°C, washed in 0.1M cacodylate buffer for 30 min and post-fixed in 1%

osmium tetroxide in 0.1M cacodylate buffer for 1 hr at 4°C. Following stepwise dehydration with increasing concentrations of ethanol and embedding in Epon 812, ultrathin sections (70nm) were stained with uranyl acetate and lead citrate and observed with a Morgagni 268D electron microscope.

Muscle tissue preparation and mitochondria isolation

The *Mtm1* knockout (KO) mouse line (genetic background 129/Sv) was generated previously (15). Mice were housed in plastic cages in a temperature-controlled environment with a 12 hr light/dark cycle and free access to food and water. The investigation complied with the Guide for the Care and Use of Laboratory Animals published by the National Institutes of Health. The animals were euthanized by rapid cervical dislocation and experiments were carefully designed to minimize the number of animals and their suffering. Muscles were treated as described previously (16). Briefly, dissected muscles were immediately frozen in liquid nitrogen-cooled isopentane and stored at –80°C or were directly solubilised with the appropriate buffer for biochemistry (protein extraction and co-immunoprecipitation) or molecular biology (RNA extraction for quantitative RT-PCR) experiments. Microsomal fractions were prepared from freshly dissected pooled *tibialis anterior* muscles from at least two mice as decribed (17). Muscles were homogenized using a Dounce homogenizer (10-15 strokes) in solution A (20 mM Na4P2O7, 20 mM Na-PO4, pH 7.4, 0.303 M sucrose, 0.5 mM EDTA, 1 mM MgCl2) supplemented by 2 mM PMSF and protease inhibitors cocktail. Homogenates were centrifuged for 15 min at 20,000 *g*, and the pellet was re-homogenized. Combined supernatants were filtered through six layers of cheesecloth and centrifuged for 15 min at 25,000 *g*. The pellet was discarded. Solid KCl was added to the supernatant, to a final concentration of 0.6 M. After centrifugation for 35 min at 200,000 *g*, the pellet was resuspended in solution B (20 mM Tris-maleate, pH 7.4, 0.303 M sucrose, 0.6 M KCl, and the same protease inhibitors as in solution A). After incubating for 1 hr, KCl-washed microsomes were pelleted for 35 min at 200,000 *g* and resuspended in solution B without KCl. All steps were performed at 4°C. Muscle mitochondria were isolated using established methods (18). Freshly dissected muscles were minced (4°C), followed by homogenization (teflon pestle) in ice-cold MSH buffer (210 mM mannitol, 70 mM sucrose, 5 mM HEPES, pH 7.4) with 1 mM EGTA. The homogenates were pelleted to remove the nuclear fraction (10 min; 680 *g* at 4°C) and the supernatant transferred to a pre-chilled tube and re-centrifuged (15 min; 6800 *g* at 4°C). The pellet was washed once in ice-cold MSH buffer (without EGTA) and used as the mitochondrial-enriched

fraction. The resulting supernatants were further centrifuged at 100,000 *g* for 30 min to generate a cytosolic fraction.

Lipid binding assays

To test the potential binding of desmin to lipids we used the PIP Strips commercial system (Echelon Bioscience Inc) according to manufacturer's instructions. Briefly, after blocking membranes with PBS with 1% non-fat-dry milk for 1 hr at RT, purified recombinant desmin was tested at increased concentrations (1μg-10 μg/ml) diluted in the same buffer and incubated in contact with PIP Strips overnight at 4°C. Bound desmin was revealed by the anti-desmin goat antibody Y20 (Santa Cruz biotechnology) followed by the peroxidase coupled Donkey anti-goat second antibody.

Phosphatase activity assays

To test the impact of desmin on MTM1 phosphoinositide phosphatase activity we performed *in vitro* and *ex-vivo* independent experiments (19). For the *in vitro* assay, recombinant GST-MTM1 fusion protein was expressed and purified as described above and mixed with purified desmin recombinant protein. The protein mixture was incubated overnight at 4°C and diluted to the final concentration of 1mg/ml in 50ml of 50 mM ammonium acetate pH 6.0. For *ex-vivo* assays, SW13vim- cells were co-transfected with desmin and MTM1 constructs (pcDNA3-desmin-Myc and pSG5-B10-MTM1) or with NF-L and MTM1 constructs (pcDNA3.1-NFL-His-Myc, and pSG5-B10-MTM1). After cell lysis the MTM1-Desmin and MTM1-NF-L complexes were immunoprecipitated using the monoclonal anti-B10 antibody. Immune-complexes were washed several times in washing buffer (see Co-immunoprcipitation part) and then in 50 mM ammonium acetate, pH 6.0. The appropriate volume of beads (1mg/ml in 50 ml ammonium acetate buffer) and recombinant protein mixtures were then assayed for phosphatase activity in 50 mM ammonium acetate pH 6.0, with either BODIPY FL-labelled phosphatidylinositol 3,5-bisphosphate and phosphatidylinositol 3-phosphate (Echelon Research Laboratories, UT USA) according to Taylor and Dixon (20). Lipids were extracted according to Blight and Dyer (21), separated on Silica Gel G60 TLC, and visualized under UV light. Phosphatase activity was also quantified after scrapping the fluorescent spots from TLC plates followed by lipid extraction and measuring the fluorescence using the Varioscan Flash (Thermo Electron Corp.) at fixed wavelengths (480/504).

Desmin solubility assays

Cells or muscles were treated as described before in co-immunoprecipitation part with the following modifications. Extracts were obtained by homogenization in extraction buffer (50 mM Tris-Cl pH 7.5, 50 mM NaCl, 5mM EDTA, 5mM EGTA, 1mM DTT, 0,5% Triton X-100, 2mM PMSF) supplemented with complete protease inhibitor tablet (Roche), 1mM Leupeptin and 1mM pepstatin A (SIGMA). Cells were homogenized with dounce homogenizer and passed five times through a 25G needle to disperse aggregates. Equal weight of *tibialis anterior* muscles were homogenized with a Dounce homogenizer in ice-cold extraction buffer supplemented with 0.05% (w/v) SDS. A cycle of 10 min homogenization spaced by 10 min incubation on ice was repeated 3 times. Cell and muscle extracts were treated by 2 cycles of freeze-defreeze in liquid nitrogen and centrifuged during 30 min at 30,000 rpm at 4°C. Pellets were collected as the insoluble material and solubilized in extraction buffer supplemented with 8M Urea.

Cytochrome oxydase, LDH and CK activities

C2C12 Cells (control and *Mtm1* KD) were grown in 6 wells plates until confluence and were trypsinized, washed twice with PBS and homogenized in HEPES extraction buffer (20 mM HEPES pH 7.4, 0,1% Triton X100, 1mM EDTA). Protein concentration was fixed at 1mg/ml and triplicates of each sample were analysed using the Cytochrome c oxydase assay kit (SIGMA) according to the manufacture's protocol. The activity of the enzyme was calculated in U/ml/g of proteins. Lactate deshydrogenase (LDH) activity was measured in the direction of pyruvate to lactate formation by following the oxidation of NADH at 340 nm (Cormay diagnostic kit). Creatine kinase (CK) activity was estimated by an enzyme linked assay, the reduction of NADPH being followed at 340 nm (Cormay diagnostic kit). All analyses were carried out at 25°C and the activities were expressed as IU per mg of muscle protein incubated. The total protein content in cardiac muscle samples was determined by the method of Bradford.

Cytochrome C release, MPT assay and ATP content

Freshly isolated mitochondria (from wild type and *Mtm1* KO mice) were washed and resuspended in MSH buffer (210 mM mannitol, 70 mM sucrose, 5 mM HEPES, pH 7.4). Equal amounts of mitochondria (2 mg protein/ml) were incubated at 25°C for 10 min with $CaCl_2$ (Ca^{2+}) to a 0.2 mM final

concentration. Small aliquots were removed to determine total cytochrome c, and released cytochrome c was determined after pelleting the remaining mitochondria (4°C; 16,000 *g* 5 min) and collecting the supernatants. To assess membrane permeability transition (MPT), swelling of mitochondria (1 mg protein/ml) was monitored in MSH buffer containing 2 mM Tris-phosphate, 5 mM succinate and 1 μM rotenone by continuous measurement of the decrease in absorbance (540 nm) using a 96-well reader (Biotek Instrument GmbH, France). A concentration of 4 nmol Ca^{2+}/mg protein was used in the measurement. All measurements were in triplicate from two independent experiments.

For ATP content**,** samples were prepared as described previously (22) with slight modifications. Equal weight of *tibialis anterior* muscles from wild type and *Mtm1* KO mice were rapidly processed for boiling in double-distilled water (10 min) followed by homogenization. ATP concentration was measured in triplicate by the Enliten® ATP Assay System (Promega Corporation, Madison, USA).

Apoptotic assays and JC-1 treatment

Cells were treated with 1 mM Staurosporine (STS, SIGMA) for 6 hr. Nuclei were analysed by confocal microscopy using Hoechst dye. TUNEL experiments were carried out using the In situ Cell Death Detection Kit, Fluorescein (Roche, France) according to the manufacturer's instructions. Mitochondrial membrane potential was assayed using the MitoProbTM JC-1 assay kit for flow cytometry (Molecular Probes, Netherlands). Cells were stained with 2 μM JC-1 for 15 min at 37°C, 5% $C0_2$, washed with PBS and analyzed by flow cytometry using 488 nm excitation with 585 emission filters.

Reverse transcription and quantitative PCR

Total RNA was purified from muscles of 2 and 5 week-old male mice and C2C12 (control and *Mtm1* KD) cells using Trizol reagent (Invitrogen) according to manufacturer's instructions. cDNAs were synthesised from 2 to 5 μg of total RNA using Superscript II reverse transcriptase (Invitrogen) and random hexamers. Quantitative PCR amplification of cDNAs was performed on Light-Cycler 480 and Light-Cycler 24 instruments (Roche) using 58°C as melting temperature. The *Gapdh* and *Mhc* gene expression were used as control because of the non-variation in their expression between wild type and *Mtm1* KO muscles or between *Mtm1* KD and control C2C12 cells. Primers are summarized in Table S2.

Statistical analysis

Throughout the paper, the distribution of data points is expressed as mean ± SEM. Statistical analysis was performed using the Mann-Whitney *U* test or the unpaired Student's test and multiple statistical comparisons between samples were performed by one-way analysis of variance followed by a Bonferroni's t-test posthoc correction to obtain a better evaluation of the variability between samples from the same group and samples from each compared group. The Statview program (version 5.0; SAS Institute Inc, Cary, NC) was used and statistical significance was set at *P < 0.05.

SUPPLEMENTARY REFERENCES

1. Biancalana, V., Caron, O., Gallati, S., Baas, F., Kress, W., Novelli, G., D'Apice, M.R., Lagier-Tourenne, C., Buj-Bello, A., Romero, N.B., et al. 2003. Characterisation of mutations in 77 patients with X-linked myotubular myopathy, including a family with a very mild phenotype. *Hum Genet* 112:135-142.
2. Penisson-Besnier, I., Biancalana, V., Reynier, P., Cossee, M., and Dubas, F. 2007. Diagnosis of myotubular myopathy in the oldest known manifesting female carrier: a clinical and genetic study. *Neuromuscul Disord* 17:180-185.
3. Buj-Bello, A., Fougerousse, F., Schwab, Y., Messaddeq, N., Spehner, D., Pierson, C.R., Durand, M., Kretz, C., Danos, O., Douar, A.M., et al. 2008. AAV-mediated intramuscular delivery of myotubularin corrects the myotubular myopathy phenotype in targeted murine muscle and suggests a function in plasma membrane homeostasis. *Hum Mol Genet* 17:2132-2143.
4. Laporte, J., Blondeau, F., Gansmuller, A., Lutz, Y., Vonesch, J.L., and Mandel, J.L. 2002. The PtdIns3P phosphatase myotubularin is a cytoplasmic protein that also localizes to Rac1-inducible plasma membrane ruffles. *J Cell Sci* 115:3105-3117.
5. Tosch, V., Vasli, N., Kretz, C., Nicot, A.S., Gasnier, C., Dondaine, N., Oriot, D., Barth, M., Puissant, H., Romero, N.B., et al. Novel molecular diagnostic approaches for X-linked centronuclear (myotubular) myopathy reveal intronic mutations. *Neuromuscul Disord*.
6. Vojtek, A.B., and Hollenberg, S.M. 1995. Ras-Raf interaction: two-hybrid analysis. *Methods Enzymol* 255:331-342.
7. Fromont-Racine, M., Rain, J.C., and Legrain, P. 1997. Toward a functional analysis of the yeast genome through exhaustive two-hybrid screens. *Nat Genet* 16:277-282.
8. Chien, C.T., Bartel, P.L., Sternglanz, R., and Fields, S. 1991. The two-hybrid system: a method to identify and clone genes for proteins that interact with a protein of interest. *Proc Natl Acad Sci U S A* 88:9578-9582.
9. Herrmann, H., and Aebi, U. 1998. Structure, assembly, and dynamics of intermediate filaments. *Subcell Biochem* 31:319-362.

10. Herrmann, H., Kreplak, L., and Aebi, U. 2004. Isolation, characterization, and in vitro assembly of intermediate filaments. *Methods Cell Biol* 78:3-24.
11. Bar, H., Strelkov, S.V., Sjoberg, G., Aebi, U., and Herrmann, H. 2004. The biology of desmin filaments: how do mutations affect their structure, assembly, and organisation? *J Struct Biol* 148:137-152.
12. Hnia, K., Hugon, G., Masmoudi, A., Mercier, J., Rivier, F., and Mornet, D. 2006. Effect of beta-dystroglycan processing on utrophin/Dp116 anchorage in normal and mdx mouse Schwann cell membrane. *Neuroscience* 141:607-620.
13. Dalkilic, I., Schienda, J., Thompson, T.G., and Kunkel, L.M. 2006. Loss of FilaminC (FLNc) results in severe defects in myogenesis and myotube structure. *Mol Cell Biol* 26:6522-6534.
14. Dorchies, O.M., Laporte, J., Wagner, S., Hindelang, C., Warter, J.M., Mandel, J.L., and Poindron, P. 2001. Normal innervation and differentiation of X-linked myotubular myopathy muscle cells in a nerve-muscle coculture system. *Neuromuscul Disord* 11:736-746.
15. Buj-Bello, A., Laugel, V., Messaddeq, N., Zahreddine, H., Laporte, J., Pellissier, J.F., and Mandel, J.L. 2002. The lipid phosphatase myotubularin is essential for skeletal muscle maintenance but not for myogenesis in mice. *Proc Natl Acad Sci U S A* 99:15060-15065.
16. Hnia, K., Hugon, G., Rivier, F., Masmoudi, A., Mercier, J., and Mornet, D. 2007. Modulation of p38 mitogen-activated protein kinase cascade and metalloproteinase activity in diaphragm muscle in response to free radical scavenger administration in dystrophin-deficient Mdx mice. *Am J Pathol* 170:633-643.
17. Rezniczek, G.A., Konieczny, P., Nikolic, B., Reipert, S., Schneller, D., Abrahamsberg, C., Davies, K.E., Winder, S.J., and Wiche, G. 2007. Plectin 1f scaffolding at the sarcolemma of dystrophic (mdx) muscle fibers through multiple interactions with beta-dystroglycan. *J Cell Biol* 176:965-977.
18. Ott, M., Robertson, J.D., Gogvadze, V., Zhivotovsky, B., and Orrenius, S. 2002. Cytochrome c release from mitochondria proceeds by a two-step process. *Proc Natl Acad Sci U S A* 99:1259-1263.
19. Rohde, H.M., Tronchere, H., Payrastre, B., and Laporte, J. 2009. Detection of myotubularin phosphatases activity on phosphoinositides in vitro and ex vivo. *Methods Mol Biol* 462:265-278.
20. Taylor, G.S., and Dixon, J.E. 2003. PTEN and myotubularins: families of phosphoinositide phosphatases. *Methods Enzymol* 366:43-56.
21. Bligh, E.G., and Dyer, W.J. 1959. A rapid method of total lipid extraction and purification. *Can J Biochem Physiol* 37:911-917.
22. Tao, G.Z., Looi, K.S., Toivola, D.M., Strnad, P., Zhou, Q., Liao, J., Wei, Y., Habtezion, A., and Omary, M.B. 2009. Keratins modulate the shape and function of hepatocyte mitochondria: a mechanism for protection from apoptosis. *J Cell Sci* 122:3851-3855.

Supplementary Figure 1

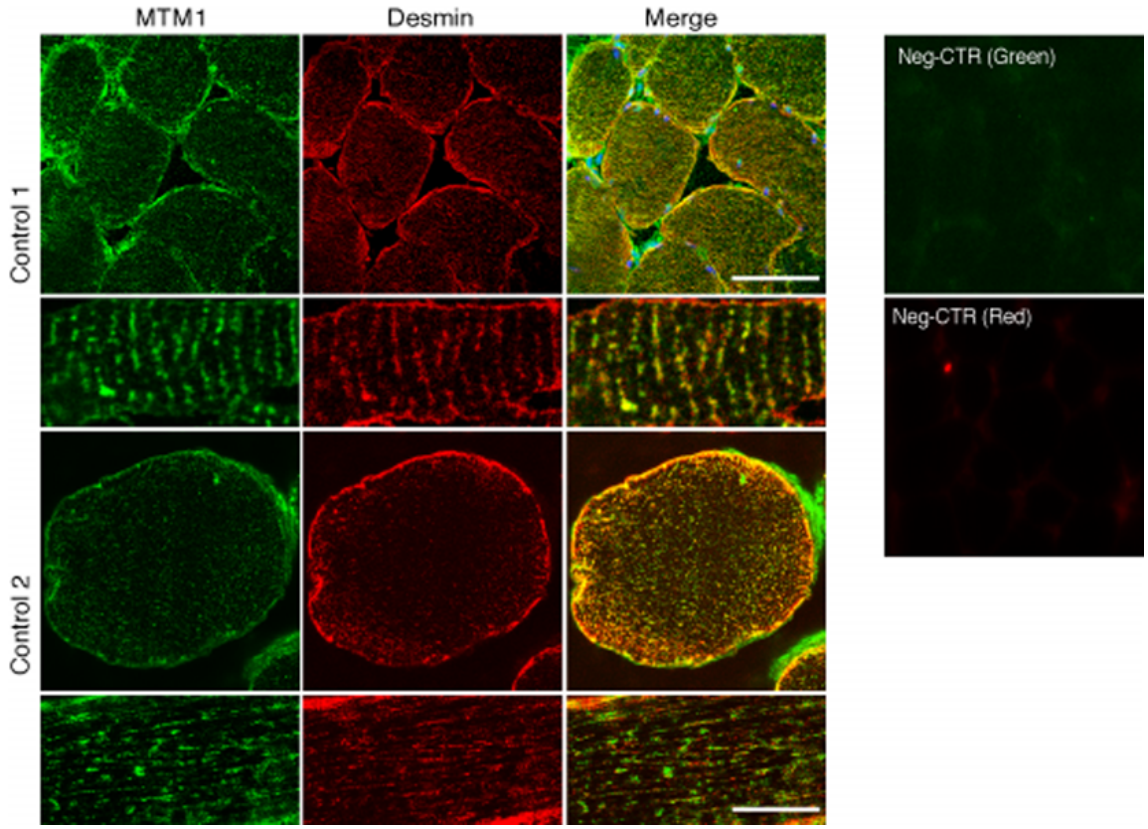

Supplementary Figure 1

MTM1 co-localizes with desmin in human muscle**.** Confocal analysis of transversal and longitudinal sections from two human control muscle biopsies (control 1 is 24 years-old and control 2 is 42 years-old) showing partial overlap between MTM1 and desmin at the sarcolemma and at the Z-disc. Scale bars = 50μm.

Supplementary Figure 2

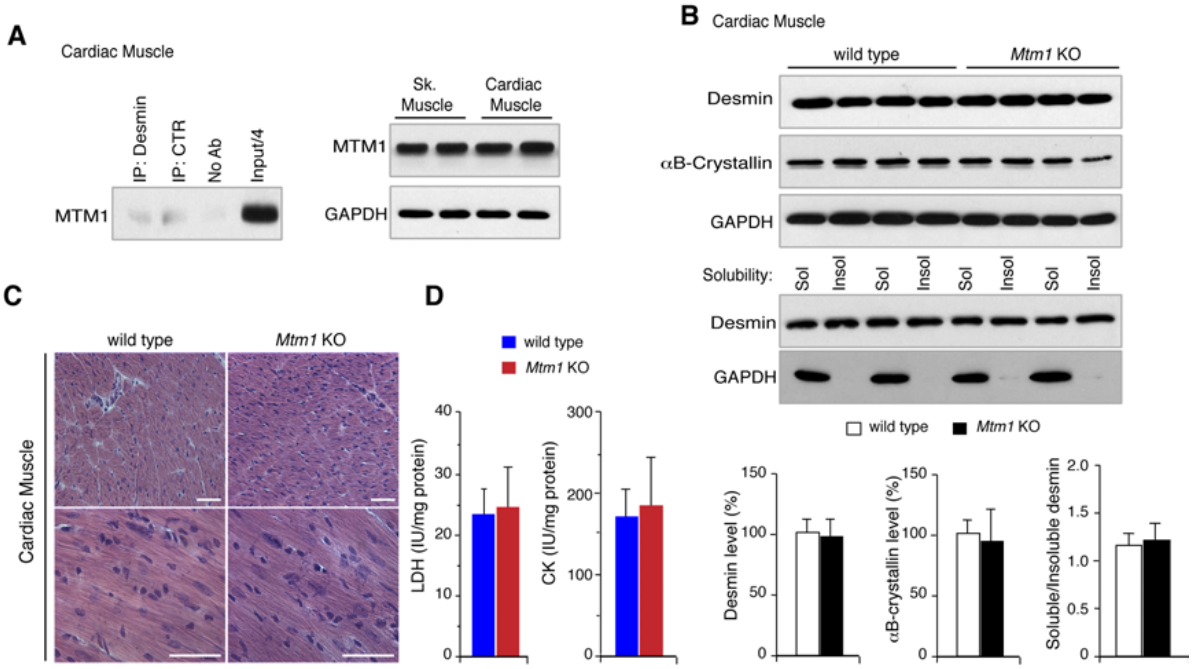

Supplementary Figure 2: (A) Desmin failed to immunoprecipitate MTM1 from cardiac muscle (right panel). Immunoblot of MTM1 in cardiac and skeletal muscle showed similar expression profile in both muscles (left panel). (**B**) Equivalent expression level of desmin and aB-crystallin in *Mtm1* vs. wild type cardiac muscle (upper panel). MTM1 knockout expression from heart did not affect desmin solubility. Sol indicates soluble fraction and Insol means insoluble material after final centrifugation (see methods) and solubilisation with 8M-urea extraction buffer (lower panel). GAPDH is a loading control. Data correlated from N=2 individual experiments and significance was set at *P< 0.05. (**C**) Transversal and longitudinal sections of wild type and *Mtm1* KO hearts stained with Haematoxylin and eosin (H&E) showed no myocardial fibrosis (myocyte injury and necrosis) in *Mtm1* KO muscle. All the analysed mice are 5 weeks old and *Mtm1* KO mice have the characterised severe muscle atrophy at that age. (**C**) LDH (lactate deshyndrogenase) and CK (creatine kinase) level in cardiac muscle from wild type and *Mtm1* KO mice. No variations were noted in these enzymes. Data correlated from two individual experiments (n=6 for wild type mice and n=7 for *Mtm1* KO mice) and significance was set at *P<0.05. Scale bars = 50μm.

Supplementary Figure 3

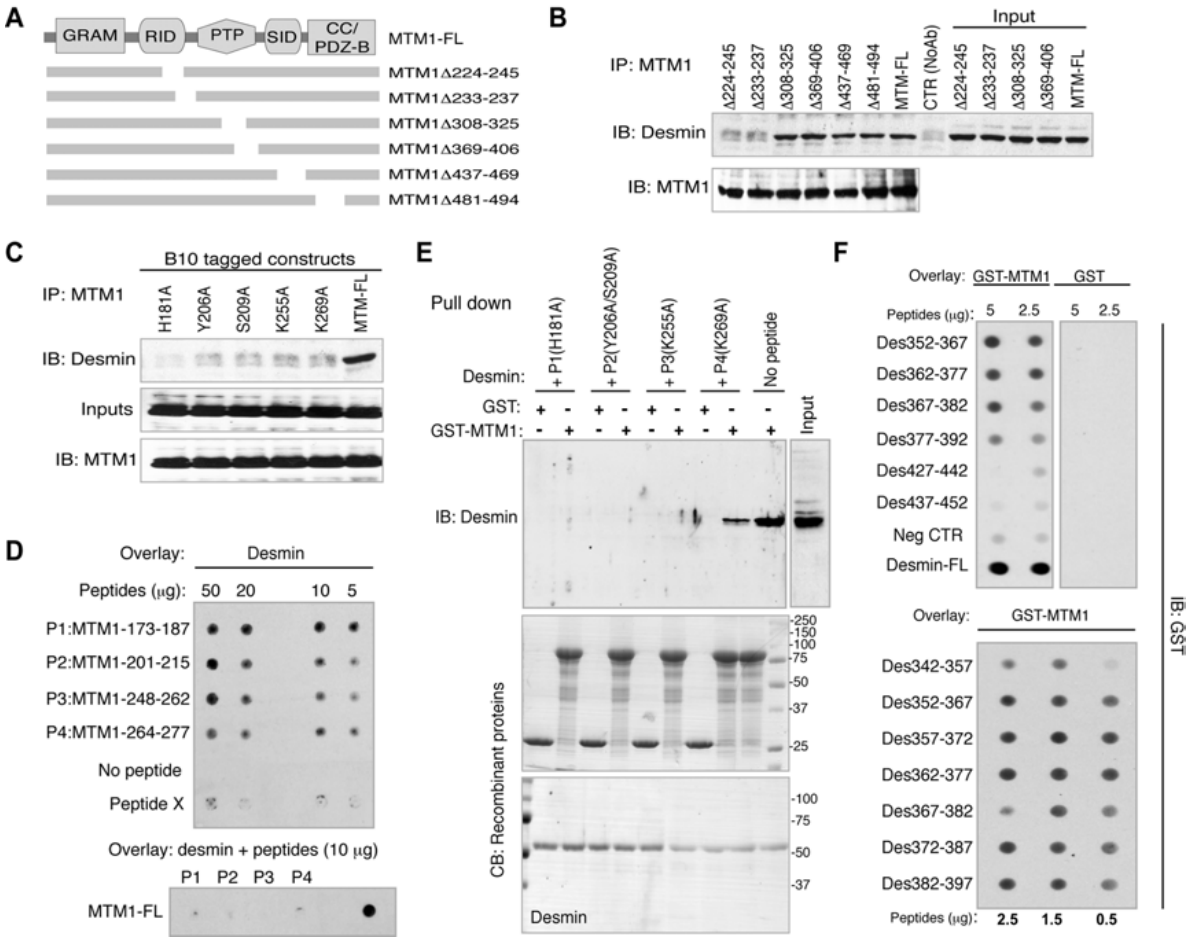

Supplementary Figure 3: Mapping the interaction domains on MTM1 and desmin**.** (**A**) Diagrammatic representation of MTM1 deletion constructs employed in co-immunoprecipitation studies. (**B**) Co-immunoprecipitation using anti-MTM1 specific antibodies was performed from co-transfected cells with desmin and MTM1 full length or specified deletion constructs. Immune-bound complexes were analysed by immunoblot with anti-desmin antibody (top panel) and MTM1 antibody (bottom panel). MTM1D224-245 and MTM1D233-237 do not interact with desmin. (**C**) Co-immunoprecipitation studies employing anti-B10 antibodies from cells lysates co-transfected with desmin and B10 tagged wild type or mutated MTM1 constructs. Immune-bound complexes were revealed with anti-desmin antibody (top panel) and anti-MTM1 antibody (bottom panel). Levels of ectopically expressed desmin are shown (middle panel). (**D**) Peptide mapping and competition to define the MTM1 binding domain. Top panel: Desmin overlay on MTM1 peptides encoding the 4 implicated loops (P1:MTM173-187, P2:MTM201-215, P3:MTM248-262, P4:MTM264-277), revealed with the desmin antibody. Bottom panel: MTM1-FL spotted on membrane was overlayed with desmin preincubated with excess of peptides (P1-P4). (**E**) Recombinant desmin alone or combined with specified mutated peptides was incubated with GST-MTM1 or GST. Coomassie blue stained gels showed GST and GST-MTM1 recombinant proteins (middle panel) and purified recombinant desmin (bottom panel) that were used for GST-pull down competition experiment. (**F**) Peptide mapping experiment using overlapping peptides of the 342-456 desmin sequence dotted on nitrocellulose membrane and overlayed by GST or GST-MTM1 recombinant proteins.

Supplementary Figure 4

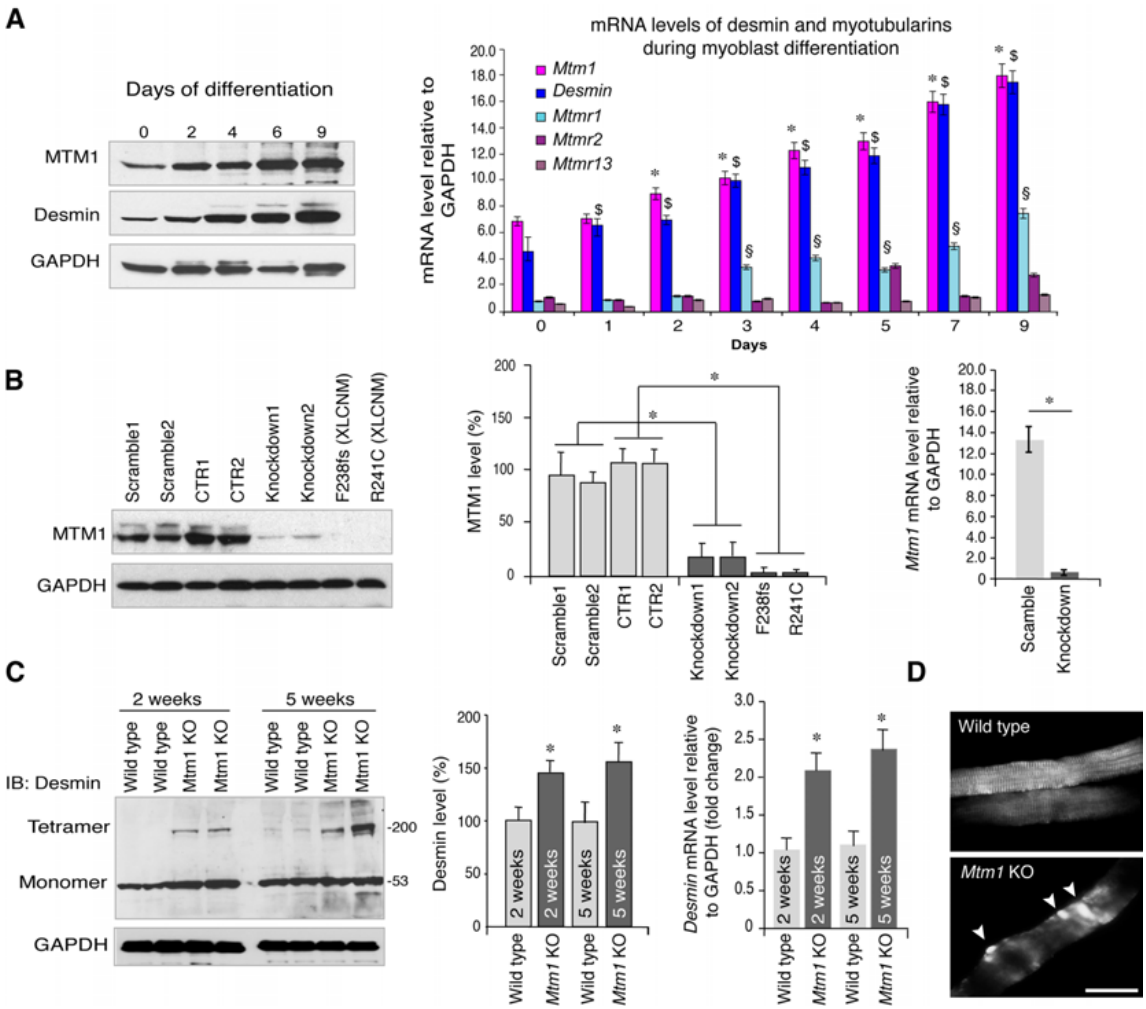

Supplementary Figure 4: Characterization of *Mtm1* knockdown C2C12 cell line and exploring desmin expression and localization in MTM1 deficient cells and muscle. (**A**) Expression of MTM1 and desmin during muscle cell differentiation employing MTM1 and desmin-specific antibodies (left panel). Quantification of mRNA levels of *desmin and Mtm1,* during myoblast differentiation was determined by quantitative RT-PCR compared to *Gapdh* or *Mhc* (right panel). (**B**) Characterization of *Mtm1* knockdown (KD) C2C12 cells. 3 clones were generated and 2 are presented here for protein and mRNA quantification comparatively to XLCNM myoblast carrying mutations leading to depletion (F238fs) or strong decrease (R241C) of MTM1 expression. Data correlated from N=3 individual experiments, n=3 separate cell culture extracts (middle and right panels) and significance was set at *P < 0.05. (**C**) Overexpression of desmin in *Mtm1* knockout (KO) muscle. Western blot analysis of muscle extracts from control and *Mtm1* KO muscles at 2 weeks and 5 weeks employing anti-desmin and anti-GAPDH specific antibodies. The 200-kDa bands detected by the desmin antibody in *Mtm1* KO muscle correspond potentially to a detergent-resistant desmin tetramer. Quantification of protein and mRNA levels of *Desmin* in control and *Mtm1* KO skeletal muscle (at 2 and 5 weeks). N= 4 individual experiments and n = 2 mice per experiment, significance was set at *P < 0.05. (**D**) Isolated fibres from *Mtm1* KO (2-weeks) muscle showed Desmin aggregates in the subsarcolemmal and intermyofibrillar compartments (arrowheads) compared to wild type muscle fibres. Scale bars represent 20μm.

Supplementary Figure 5

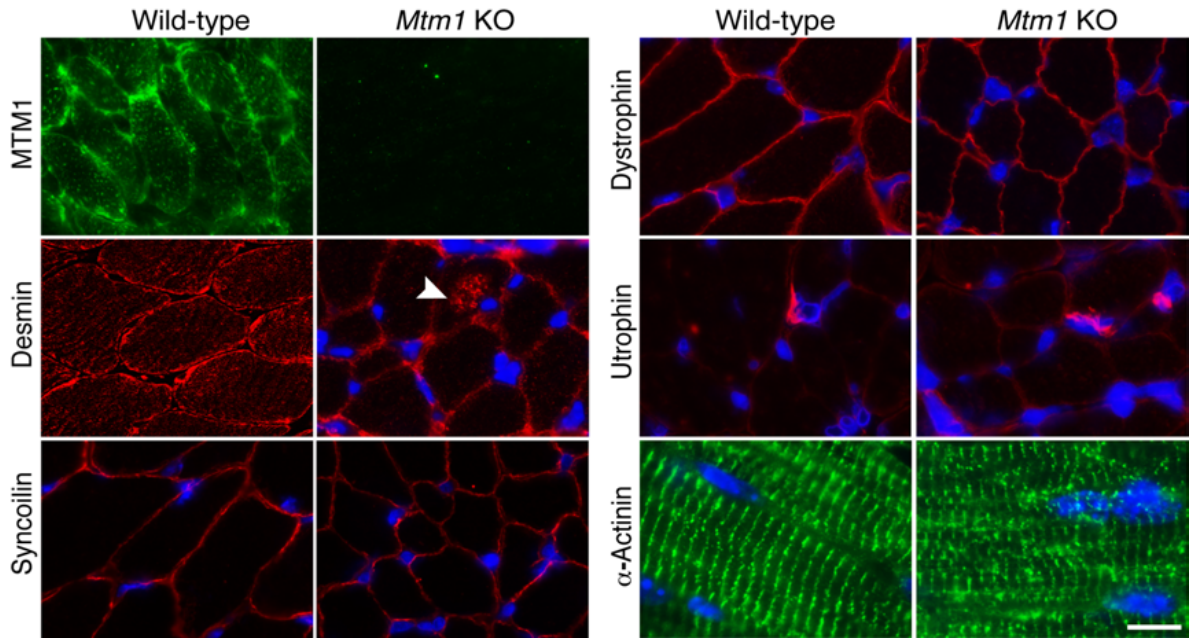

Supplementary Figure 5: Specific accumulation of desmin in *Mtm1 KO* muscle. Immunolocalisation of syncolin, dystrophin, utrophin, a-actinin (Z-disc protein) and titin (M-line protein) in 2-week old control and *Mtm1* KO muscles. Accumulation of desmin was observed in *Mtm1* KO muscle fibers (arrowheads) but not the other tested protein. Scale bars represent 20μm.

Supplementary Figure 6

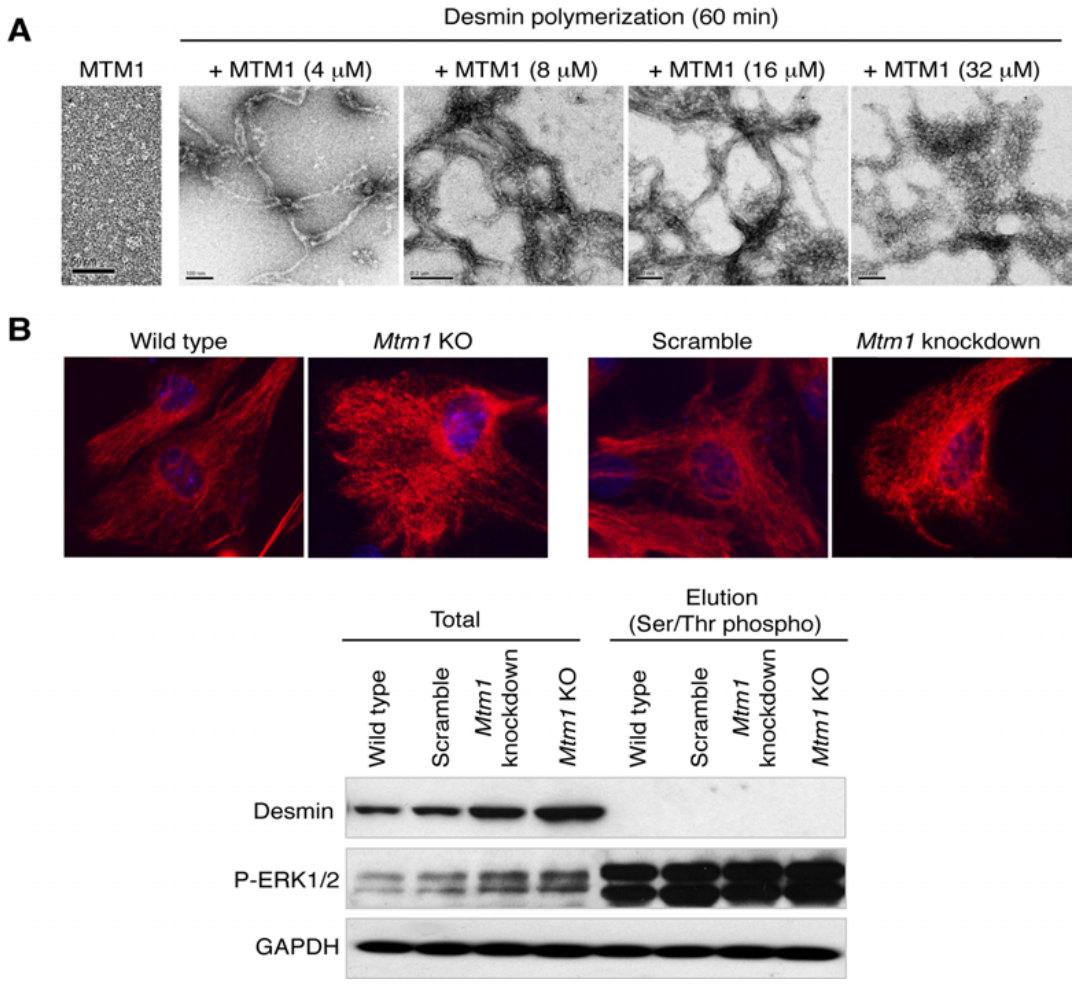

Supplementary Figure 6: Impact of MTM1 on desmin filaments assembly**.** (**A**) MTM1 affects desmin filament structure. Recombinant desmin (10 μM) was mixed with increasing concentrations of recombinant MTM1 (cleaved from GST tag) and desmin filament assembly was monitored by electron microscopy after 60 min of assembly. Addition of MTM1 (4 μM) led to the formation of ribbon-like, bifurcating and branching filaments with more variable width and length. Excess of MTM1 (8-32 μM) inhibit completely filaments formation. (**B**) Desmin filament collapse/aggregation in *Mtm1* KO and knockdown myoblasts is not promoted by desmin phosphorylation. Immunoblot of desmin before (Total) and after elution from Ser/thr Phospho-enrichment column. ERK1/2 and GAPDH were analysed as positive and loading controls, respectively.

Supplementary Figure 7

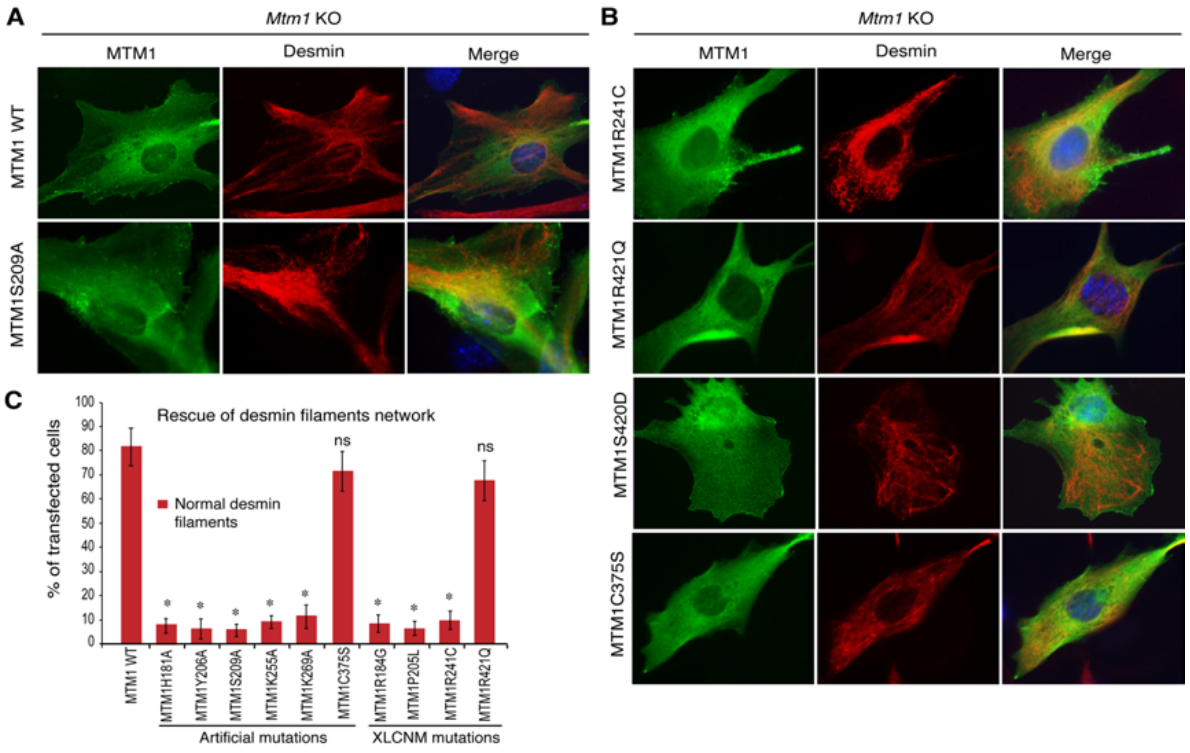

Supplementary Figure 7: Rescue of desmin filaments in *Mtm1* KO myoblasts. (**A**) Overexpression of wild type MTM1 but not mutated constructs (in the interaction sites with desmin) re-establishes normal desmin filament network in *Mtm1* KO myoblast (see also supplementary figure 7A). (**B**) XLCNM mutation R421Q and the artificial mutations S420D and C375S could re-establish normal desmin filament in *Mtm1* KO cells but not the XLCNM mutation R241C, suggesting that only MTM1 mutations situated in the interaction sites with desmin are not able to rescue desmin filaments network. (**C**) Quantification of the impact of all tested MTM1 mutations on filament network in *Mtm1* KO cells. Approximately 100 transfected cells were counted over 3 independent experiments. The significance was set at *P<0.05.

Supplementary Figure 8

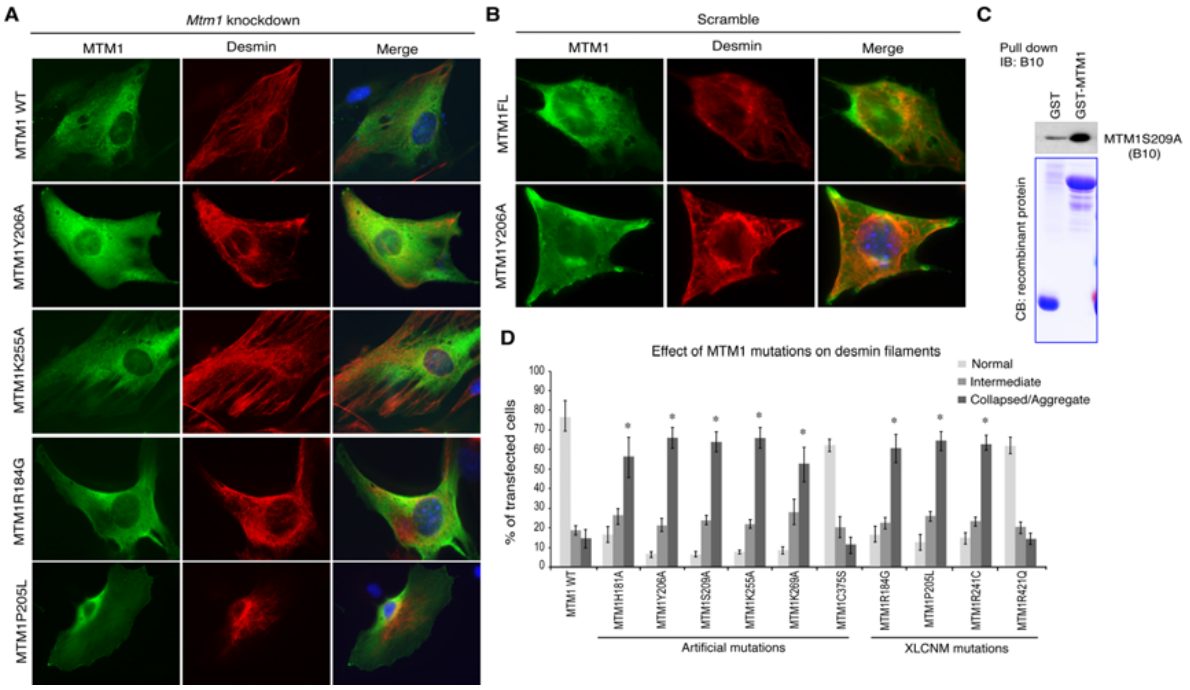

Supplementary Figure 8: Effects of MTM1 mutations on desmin filaments (**A**) Overexpression of wild type MTM1 but not mutated constructs (in the interaction sites with desmin) re-establishes normal desmin filament network in *Mtm1* Knockdown cells similarly to *Mtm1* KO cells (Supplementary Figure 7). (**B**) Overexpression of wild type MTM1 does not impact on desmin network in control C2C12 cells (Scramble) but overexpression of mutated MTM1 proteins carrying point mutations within the interaction sites with desmin (artificial or patient's mutations) lead to collapsed/aggregating desmin filaments. These mutated proteins may promote a dominant negative effect by binding the endogenous MTM1 protein (**C**) and disrupting its interaction with desmin. Quantification of the impact of MTM1 mutations on filament network in C2C12 cells. Approximately 80 to 100 transfected cells per experiment were counted over 3 independent experiments. The significance was set at *P<0.05.

Supplementary Figure 9

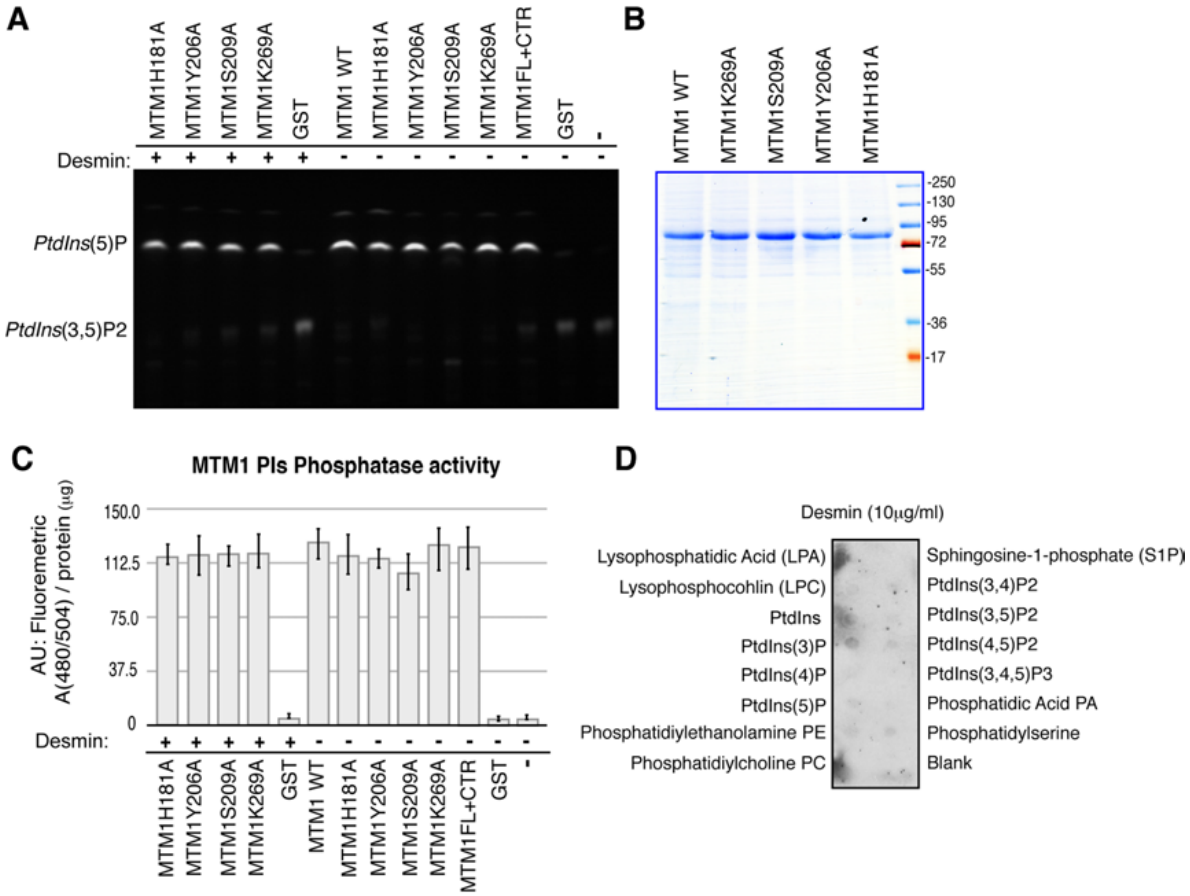

Supplementary Figure 9: Impact of MTM1 mutations in the desmin interaction sites on PIs phosphatase activity in vitro. (**A**) PtdIns(3,5)P_2 dephosphorylation to PtdIns5P by wild type or mutated MTM1 constructs (H181A, Y206A, S209A and K269A) alone or combined to desmin recombinant protein. (**B**) Coomassie blue stained gel of the MTM1 GST-fusion constructs employed for the enzymatic assay (right panel). (**C**) Quantification of the phosphatase activity: intensities of PtdIns5P and PtdIns(3,5)P_2 spots were measured at A(480/504) and expressed as a ratio on the recombinant protein quantity. Fluorometric measurements were made twice and their averages were used. Data correlated from two individual experiments and significance was set at *P<0.05. (**D**) Desmin did not bind directly to lipids. A fat blot of specified lipids was overlayed with recombinant desmin (10 µg/ml), followed by probing with desmin specific antibodies.

Supplementary Figure 10

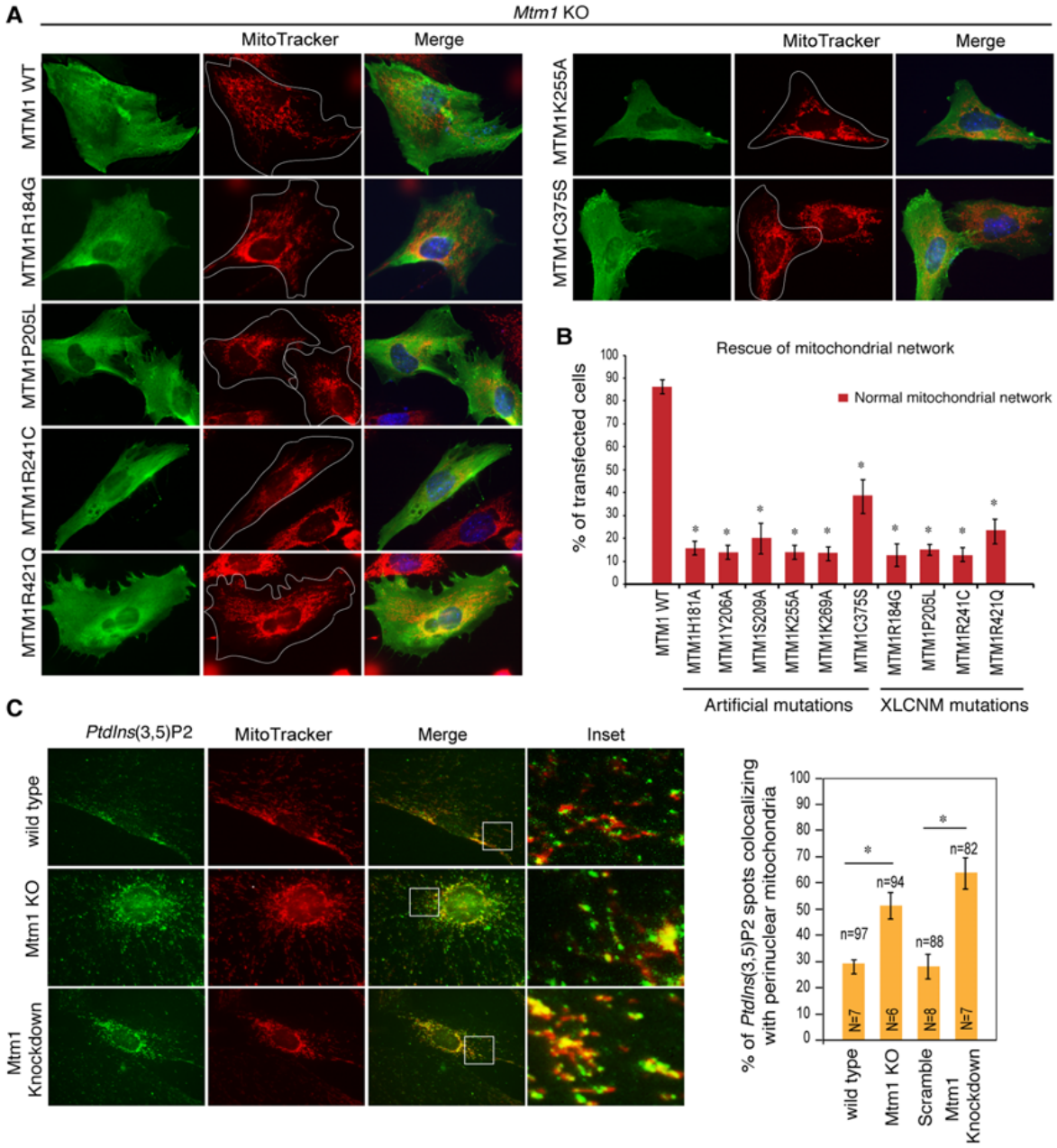

Supplementary Figure 10: (**A**) MTM1 mutations fail to restore mitochondria network in *Mtm1* KO cells. Overexpression of wild type MTM1 but not mutated constructs (artificial and XLCNM mutations) did not rescue mitochondrial shape/network in *Mtm1* KO myoblast. (**B**) Quantification of the impact of MTM1 mutations on mitochondrial shape in *Mtm1* KO cells compared to MTM1 wild type (WT). Approximately 150 transfected cells were counted over 2 independent experiments. The significance was set at *P<0.05. (**C**). PtdIns(3,5)P_2 immunodetection in wild type and *Mtm1* KO/knockdown cells showed a similar profile as mitochondria. Perinuclear accumulation of PtdIns(3,5)P_2 and mitochondria in MTM1 deficient cells showed also partial overlapping between the PI and MitoTracker, suggesting a potential role of MTM1 substrate PtdIns(3,5)P_2 in mitochondrial homeostasis or a cytotoxic effect of PI accumulation on mitochondrial function.

Supplementary Figure 11

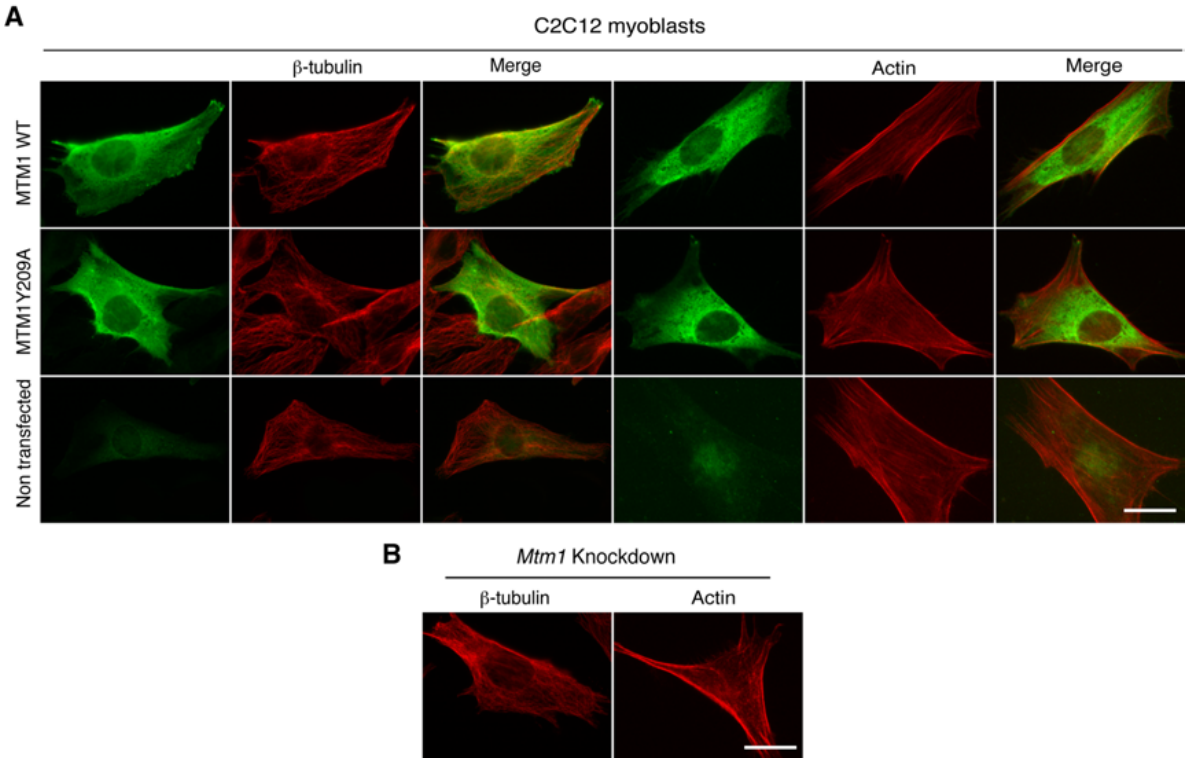

Supplementary Figure 11. Disruption of MTM1-Desmin interaction does not impact on MTs and MFs networks. (**A**) Overexpression of wild type or mutated MTM1 constructs (that did not bind desmin) in C2C12 cells did not affect microtubules (MTs) and actin filaments (MFs) architecture. C2C12 cells tranfected with specified B10-tagged MTM1 constructs were processed with anti-B10 and anti-β tubulin or anti-actin antibodies. (**B**) The morphology of MTs and MFs of *Mtm1* KD C2C12 cells. Scale bar=50 μm.

Supplementary Figure 12

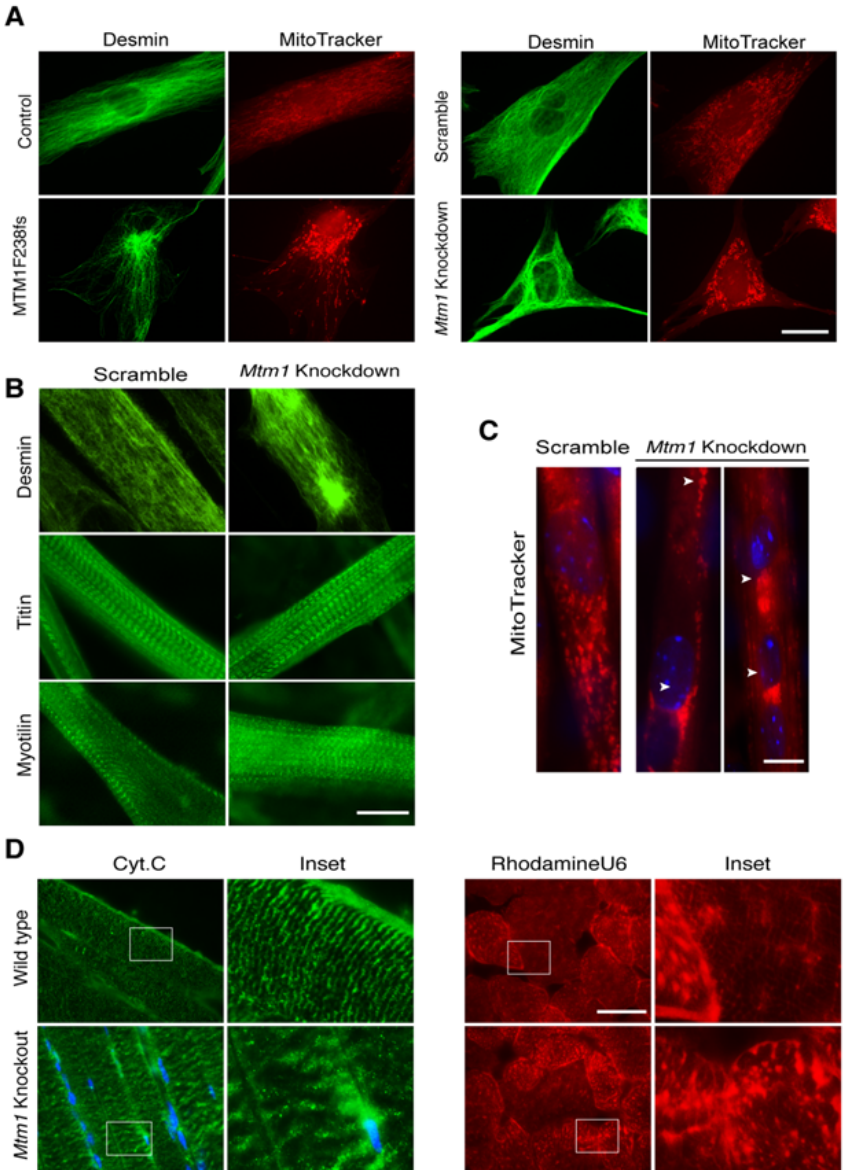

Supplementary Figure 12: (**A**) Desmin and mitochondria collapse in XLCNM patient myoblasts, *Mtm1* knockdown cells and *Mtm1* KO muscle. Control vs. MTM1F238fs patient myoblasts and scramble vs. *Mtm1* KD cells were processed for imaging following incubation with MitoTracker red and anti-desmin specific antibodies. Desmin and mitochondria collapsed around nuclei in XLCNM and *Mtm1* KD C2C12 cells. (**B**) Desmin aggregates were present in *Mtm1* KD myotubes. Control or *Mtm1* KD C2C12 myotubes were processed for imaging with anti-desmin, anti-titin or anti-myotilin specific antibodies. Desmin formed aggregates in KD cells whereas, titin (A-I line) and myotilin (z-line) showed similar localisation between control and *Mtm1* KD myotubes. Scale bar=50 μm. (**C**) Mitochondria network is also altered in *Mtm1* KD myotubes with a specific accumulation between nuclei myotubes (arrowheads). Scale bar=50μm. (**D**) Subsarcolemmal and intermyofibrillar mitochondria are disorganised in *Mtm1* KO muscles. Longitudinal muscle sections from control and *Mtm1* KO mice were probed with anti-cytochrome *c* antibody. Mitochondria accumulation was detected in muscle transversal sections from *Mtm1* KO mice after injection with the RhodamineU6 probe. Scale bars=50 μm.

Supplementary Figure 13

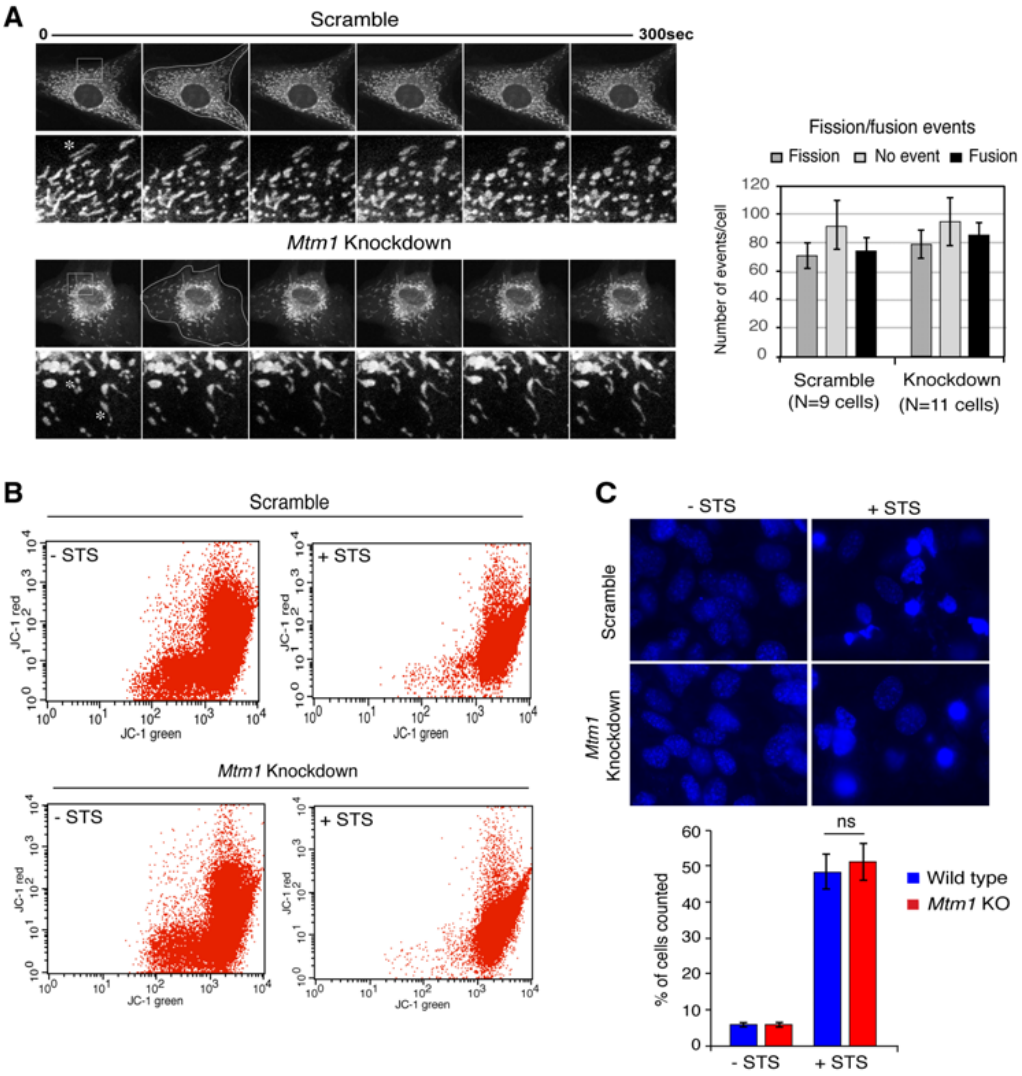

Supplementary Figure 13: Mitochondrial fission/fusion and susceptibility to apoptosis in *Mtm1* Knockdown cells are not affected. (**A**) Mitochondrial dynamics of control and *Mtm1* KD C2C12 cells were monitored over 300 sec by time-lapse microscopy (left panel). Quantification of mitochondrial fission and fusion events in control and *Mtm1* KD C2C12 cells (right panel). Mitochondria were counted individually in 3 distinct regions of the cell. Around 50 mitochondrial entities were scored as dividing (fission) or fusing (fusion) or neither (no event) per region from 9 control C2C12 cells (N=9) and from 11 *Mtm1* KD cells (N=11). Data correlated from 2 independent experiments and significance was set at *P < 0.05. (**B**) *Mtm1* KD did not impact on mitochondrial transmembrane potential. Control and *Mtm1* KD C2C12 cells were incubated with JC-1 and were analysed by FACS. Samples previously treated with 1mM staurosporine (STS) were also included in the assay. No significant shift in the profile of control versus *Mtm1* KD samples was observed. (**C**) Knockdown *Mtm1* in muscle cells did not increase susceptibility to apoptotic events. Control and *Mtm1* KD C2C12 cells were treated with (STS) and the morphology of their nuclei (stained with Höechst) was analysed by confocal microscopy (left panel). Cells with condensed or fragmented DNA (with or without STS treatment) were scored (right panel). Data correlated from 2 independent experiments using 4 different cell batches. Approximately 120 cells were counted for each sample and significance was set at *P < 0.05.